Energy & Buildings

A framework for a multi-sourced, data-driven building energy management toolkit

--Manuscript Draft--

Manuscript Number:	ENB-D-21-00485
Article Type:	Full Length Article
Section/Category:	HVAC
Keywords:	Building energy management; Multi-source data analytics; Change point models; Inverse energy modelling; Clustering
Corresponding Author:	Andre Arifin Markus, B.Eng Carleton University Department of Civil and Environmental Engineering Ottawa, Ontario CANADA
First Author:	Andre A. Markus
Order of Authors:	Andre A. Markus
	Brodie W. Hobson
	H. Burak Gunay
	Scott Bucking
Abstract:	Poor building energy performance often arises from suboptimal operations such as inappropriate control sequences or hard faults in heating, ventilation, and air-conditioning (HVAC) systems. Furthermore, such deficiencies are often left unaddressed due to a lack of accessible analytical tools that can derive insights which identify energy-saving measures using multiple data resources. This paper presents a novel multi-source data-driven energy management toolkit as a synthesis of established inverse energy modelling, anomaly detection and diagnostics, load disaggregation, and occupancy and occupant complaint analytics methods in the literature. The toolkit contains seven functions that input HVAC control, energy meter, Wi-Fi-based occupancy, and work order log data to detect hard and soft faults, improve sequences of operation, and monitor energy flows, occupancy patterns, and occupant satisfaction. The toolkit's unique multifaceted analytical approach was demonstrated on a case study building as a proof of concept and the generated insights were used to identify operational deficiencies stemming from inappropriate overheating setpoints and perimeter heating devices. The function library along with the data from the case study were made publicly available as supplemental files to this paper [1].
Suggested Reviewers:	Bing Dong The University of Texas at San Antonio bing.dong@utsa.edu
	Zheng O'Neill The University of Alabama zoneill@eng.ua.edu
	Clayton Miller National University of Singapore Faculty of Design and Environment: National University of Singapore School of Design and Environment clayton@nus.edu.sg
	Tianzhen Hong Lawrence Berkeley Laboratory: E O Lawrence Berkeley National Laboratory thong@lbl.gov
	Mary Ann Piette Lawrence Berkeley Laboratory: E O Lawrence Berkeley National Laboratory MAPiette@lbl.gov
Opposed Reviewers:	

Cover Letter

Andre Markus
MASc. Candidate
Department of Civil and Environmental Engineering
Carleton University, Ottawa, Canada

February-23-21

Jianlei Niu and Mattheos Santamouris
Editors-in-Chief, Energy and Buildings

Dear Profs. Niu and Santamouris,

Please find in this package our submission for consideration to be published in Energy and Buildings. Our paper is titled, "A framework for a multi-sourced, data-driven building energy management toolkit". The paper is motivated by the apparent lack of accessible analytical building energy management tools which derive energy-saving insights from multiple streams of operational data. This paper proposes a framework for a multi-sourced, data-driven toolkit as a synthesis of established inverse energy modelling, anomaly detection and diagnostics, load disaggregation, and occupancy and occupant complaint analytic approaches in the literature. The toolkit's capability is demonstrated on an academic building in Ottawa, Canada. The toolkit, as a set of seven Python functions, is open-sourced and available on GitHub. We believe the proposed framework will form the basis from which other researchers may base derivations of similar toolkits. Energy and Buildings serves catalyst to endeavouring new concepts and enables researchers to share and spawn inspiration.

Should you have any questions or further requests about this submission, please feel free to contact me.

Regards,
Andre Markus, B.Eng.

Corresponding Author: Andre Markus

Main Address:

Carleton University

Department of Civil and Environmental Engineering

1125 Colonel By Drive

Ottawa, Ontario, Canada K1S 5B6

Email: andre.markus@carleton.ca

Tel: +1 416 828 5270

A framework for a multi-sourced, data-driven building energy management toolkit

Andre A. Markus[1], Brodie W. Hobson[1], H. Burak Gunay[1], Scott Bucking[1]

[1]Department of Civil and Environmental Engineering, Carleton University, Ottawa, Canada

Abstract

Poor building energy performance often arises from suboptimal operations such as inappropriate control sequences or hard faults in heating, ventilation, and air-conditioning (HVAC) systems. Furthermore, such deficiencies are often left unaddressed due to a lack of accessible analytical tools that can derive insights which identify energy-saving measures using multiple data resources. This paper presents a novel multi-source data-driven energy management toolkit as a synthesis of established inverse energy modelling, anomaly detection and diagnostics, load disaggregation, and occupancy and occupant complaint analytics methods in the literature. The toolkit contains seven functions that input HVAC control, energy meter, Wi-Fi-based occupancy, and work order log data to detect hard and soft faults, improve sequences of operation, and monitor energy flows, occupancy patterns, and occupant satisfaction. The toolkit's unique multifaceted analytical approach was demonstrated on a case study building as a proof of concept and the generated insights were used to identify operational deficiencies stemming from inappropriate overheating setpoints and perimeter heating devices. The function library along with the data from the case study were made publicly available as supplemental files to this paper [1].

Keywords: Building energy management; Multi-source data analytics; Change point models; Inverse energy modelling; Clustering.

1.0 Introduction

Buildings often exhibit significant discrepancies between predicted and actual energy performance, largely attributable to suboptimal and uninformed operations, with reports of buildings consuming substantially more energy than predicted during the design phase [2]–[7]. The lack of accessible operations management solutions that derive insight and feedback contributes to this 'performance gap'. There is great potential for operational improvements as operations account for 80% to 90% of a building's life-cycle energy consumption [8], with over

half of that consumed by heating, ventilation, and air conditioning (HVAC) systems [9], [10]. Despite ample resources and tools to support energy optimization in the design phase, methods to supplement energy optimization efforts during existing buildings' operational phase lack substantiation and standardization. Improvements to the operation of buildings can result in overall annual energy savings of up to 30% [11]–[13], and presents considerable opportunities for energy-savings in a wide variety of existing buildings [14]. Furthermore, energy audits – which are traditionally performed to inform energy-saving measures – are often time-consuming, scarcely executed, and can ultimately be cost prohibitive to maintain continual energy savings [15], while a software-based operation-centric solution that is integrated into the existing building controls and operation data infrastructure can be implemented with relatively low effort. Thus, methods to improve buildings performance through better operation are promising for addressing the performance gap in existing buildings. This paper presents a multi-source data-driven energy management toolkit as a synthesis of established data-driven approaches to operational analytics in the literature. The capabilities of the toolkit were demonstrated on a case study building in Ottawa, Canada.

1.1 Background and previous work

Data-driven approaches for building operation are prevalent in the literature. Moreover, the growing practice of archiving long-term operational data presents potential for operation analytics [16]. Common examples of these data sources include energy meter data, HVAC control network data from the building automation system (BAS), Wi-Fi-based device count data from IT networks, and computerized maintenance management system (CMMS) data containing occupant complaints and work order logs.

Research using meter data have gravitated towards developing data-driven models to establish an energy use baseline, detect energy use anomalies, and make energy use forecasts. Though typically used by energy service companies (ESCOs) to quantify energy savings achieved through a retrofit, baseline energy modelling can also be used to detect and interpret energy use anomalies and act as an energy performance benchmark. Zhang *et al.* [17] compared four popular baseline modelling approaches and their ability to predict HVAC heating energy consumption, noting the benefit and comparable predictive accuracy of simple change-point regression models to that of physics-based models. Gunay *et al.* [18] compared three inverse modelling approaches using heating and cooling

loads, finding that nearly half the buildings tested in the study did not have a weekly air handling unit (AHU) operating schedule. The complex and multi-faceted behaviour of building energy often solicits the use of such regression models to accurately establish energy baselines and forecast energy consumption [17], [19]. Meter data have also been used to develop methods for energy end-use disaggregation. Most meter networks in existing buildings lack the resolution to understand major energy end-uses and their flows within a building. Though prevalent in the residential setting [20]–[22] to disaggregate energy use by appliances, its application and insight have seldom extended to large-scale commercial buildings. For example, Akbari [23] developed an end-use disaggregation model using meter data, temperature dependent load regression coefficients, and simulated end-use models to disaggregate hourly building electricity consumption into its major end-uses. Ji *et al.* [24] presented a Fourier series-based model to disaggregate electricity consumption into light and plug-in, HVAC, and other miscellaneous loads such as elevators in office buildings and shopping malls. Doherty and Trenbath [25] used smart plug submetering to assess the viability of a model to disaggregate individual plug-in loads of typical office equipment and its correlation to the building's plug load submeter data. Operators of commercial buildings with access to limited submetering data are unable to discern the distribution of energy within the building. This insight can be useful for isolating energy use anomalies to specific end-uses from bulk meter data.

Research using HVAC control network data has been focussed on developing methods for automated fault detection and diagnosis (AFDD) and predictive controls, and efforts to improve the usability of HVAC control network data in AFDD and predictive controls at scale has led to the development of new metadata schemas and automated metadata inference algorithms. AFDD approaches have been intended to identify common hard faults in a building's HVAC system (e.g., stuck AHU dampers and valves, etc.) and common soft faults (e.g., a lack of an AHU operating schedule [26], [27], etc.). Kim and Katipamula [28] categorized several AFDD studies by their methods, noting that process-history based AFDD approaches, whereby archived performance data is used to estimate the parameters of inverse models, were the most popular. These studies were further subdivided into two groups, grey-box and black-box model-based methods, with the latter often deriving parameters with no physical implication [28]. A recent review article by Shi and O'Brien [27] noted that black-box methods were especially appealing to researchers due to

their flexibility and ease of development, though the challenge becomes how to present AFDD results to building operators in such a way to intuitively foster energy-saving decisions [29]. Model-based predictive control (MPC) is another subfield of operational data analytics using HVAC controls data. Gunay *et al.* [30] reviewed several indoor climate control strategies in the literature including MPC, noting its ability to generate optimal controls outputs given constraints over a prediction horizon and its applications of different forms of MPC to zone-, system-, and plant-level HVAC equipment. Afram and Janabi-Sharifi [31] concluded that most MPC approaches are based on steady-periodic linear models of the system, and can incorporate various factors related to energy cost and consumption as well as external factors such as weather and occupancy, allowing for a robust implementation in HVAC systems. Simulated and experimental system-level applications have been demonstrated to reduce energy consumption by ~20% [32]–[34]. There are, however, notable disadvantages to data-driven AFDD and MPC models derived from such large datasets. They require large quantities of high quality and high temporal resolution data under a wide range of operating conditions to function optimally, and their accuracy and reliability is heavily influenced by the quality of data [35]. Thus, the implementation of such data-driven approaches constitutes cleaning the data, such as removing stagnant values and outliers due to faulty sensors and temporary network communication issues, for example.

Though metadata models such as Project Haystack and Brick exist, the seldom implementation of a standardized data labelling terminology or format [36] also presents a major obstacle for data-driven approaches using HVAC controls data. As BASs in most existing buildings do not follow a standard metadata model, BAS metadata need to be inferred by human experts from labels, graphics, and as-built drawings prior to the deployment of data-driven energy management algorithms for AFDD, predictive controls, etc. As this is a manual and labour-intensive process, an active research area centers on developing metadata inferencing algorithms which can automatically classify labels by type and associate them by their functional relationship [37]–[40].

In recent years, Wi-Fi device count data have been recognized as a promising proxy to estimate occupancy levels in commercial buildings [41], [42]. Research using Wi-Fi device count data has been used in guiding occupant-centric control (OCC) algorithms. Wi-Fi data presents a non-intrusive approach to infer occupancy metrics with relatively flexible applicability [43]. Wang *et*

al. [43] developed and tested a Wi-Fi based occupancy model employing an ensemble modelling technique, specifically random forest, noting its high accuracy and ability to integrate with existing Wi-Fi infrastructure. Zhao *et al.* [44] developed a real-time occupancy detection model at the zone- and room-level using a Bayesian belief network (BBN) which incorporated a fusion of physical occupancy sensors with Wi-Fi and GPS data. Similarly, Longo *et al.* [45] developed an occupancy estimation model using Wi-Fi data and Bluetooth connectivity. Wi-Fi data has been used in concert with Bluetooth or GPS data to refine its estimation accuracy, though arguably, archived Wi-Fi data is more prevalent in buildings and would not require additional sensors. Implementation of such occupancy-based models has generally gravitated towards HVAC controls due to their demonstrated effectiveness to reduce energy consumption [46]–[52]. Park *et al*. [53] reviewed several occupancy-driven approaches to building controls, noting key occupancy indicators such as count, arrival time, and departure time, albeit few used Wi-Fi data. Zou *et al.* [54] implemented a predictive light dimming algorithm which derived occupants' presence and occupant count using Wi-Fi data to dynamically adjust lighting conditions based on occupant count and location, resulting in a 93% lighting energy saving from traditional lighting schedules in a commercial building. Balaji *et al.* [55] presented a predictive model for AHU outdoor air damper operations using Wi-Fi for high resolution occupancy data, resulting in HVAC electricity savings of ~18%. Though it should be noted that Wi-Fi data, as with any signal propagating medium, can suffer from dead-zones which will inhibit estimation accuracy [56]. Privacy is another concern which may cause reluctance in implementation of these models.

Albeit scarce in the practice, computerized maintenance management system (CMMS) data in the form of complaint logs and work orders have been analyzed and used to identify anomalous zones and malfunctioning equipment. Occupant temperature complaints are commonly symptomatic of faulty HVAC operation though often the corrective course of action for operators is to change temperature setpoints [57]. While this change may satisfy the individual complainant, it may dissatisfy the larger group. In this case, the problem may be more suitably attributed to an anomaly with the particular zone. Dutta *et al.* [58] employed association rule mining to extract hot/cold complaints and explored the spatiotemporal relationship of the complaints to detect anomalous zones. More recently, the same method was used to infer building performance metrics from tenant surveys [59]. Gunay *et al.* [60] proposed a complaints-based algorithm to extract insights into

maintenance performance of building systems and components. The greatest challenge in using CMMS data is the interpretation of such a large and unstandardized dataset. Thus, use of this type of data solicits ample preprocessing.

In the past two decades, research fields using operational data have gained popularity with the increased practice of archiving operational data. However, these data sources have been largely treated as disparate. Thus, previous attempts at developing a data-driven building energy management solution often focused on a single domain of data analytics. For instance, the Commercial Building Energy Saver (CBES) presented by Hong *et al.* [61] is intended to assess building performance pre- and post-retrofit and help owners make optimal retrofit decisions. Besides geometrical and construction parameters, the toolkit relies exclusively on electricity and gas usage for baseline energy benchmarking. Costa *et al.* [62] formulated a toolkit built upon previous efforts in data-driven strategies using HVAC controls data to derive operational modes, though ultimately focused on AFDD. Zhang *et al.* [63] developed an open-sourced toolkit that synthesized existing occupant detection devices and analyzed occupancy patterns which can be used to tailor operating schedules; this toolkit was limited to OCC. BETTER by Li *et al.* [64] and FirstView by the New Buildings Institute [65] both offer a data-driven toolkit employing inverse modelling to benchmark building energy consumption, disaggregate end-uses, and identify energy-saving measures, though both limit derivations of energy-saving insight from energy use data. The disadvantage of restricting analysis to one operation data source is that it effectively constricts the generated insight from the toolkit to a single approach to energy savings. Ultimately, there are multiple avenues for energy-saving that would go unnoticed and ample energy-saving potential untapped.

Ample benefits exist in integrating various operational data sources for operational analytics [66]. The intricate and interdependent nature of building operations is such that inefficiencies or anomalies in one domain may translate to others [27]. Multi-source operational analytics can be used to derive additional or refine existing energy-saving insight by establishing functional relationships between multiple domains. For example, combining energy meter data with HVAC controls network data can be used disaggregate end-uses and identify faulty equipment. Gunay *et al.* [67] employed linear regression models using HVAC controls data to characterize the

operational state of major energy systems, which enabled high accuracy disaggregation of end-uses at low temporal resolution meter data. Disaggregation produced an accurate representation of the specific components' power draw and the insights generated can be used to focus fault detection efforts into specific equipment rather than an entire system. Integrating occupancy data with energy meters can disaggregate energy loads to individual occupants' plug-in loads. Rafsanjani and Ahn [68] presented a cluster-based approach to associate occupancy events with power fluctuations using Wi-Fi and electricity load meters. Their approach was tested in two commercial buildings and was used to infer occupancy using power fluctuations from a predetermined baseline power consumption and entry/exit events. Approaches featuring this blend of data can be used to garner a more granular awareness of occupant behaviour and disaggregate electricity loads to occupant's plug-in and lighting loads. HVAC and occupancy data can be used to identify inefficiencies in outdoor airflow control and scheduling. Hobson *et al.* [69] developed and tested a cluster analysis-based approach focusing on occupancy via Wi-Fi data; classification trees intended to project day-ahead occupancy based on day type were employed using motifs from lighting and plug-in loads. The case study on the academic building exposed chronic overventilation, well above what was required for the projected occupancy. This insight was used to tailor occupant-centric schedules and ventilation rates. Combining CMMS and HVAC data show promise in identifying system conditions that trigger hot/cold complaints. Gunay *et al.* [70] modelled the frequency of complaint-driven temperature setpoints adjustments with concurrent indoor and outdoor temperature data. Their investigation revealed two distinct optimal temperature setpoints that minimize thermal complaints during the heating and cooling seasons separately. Evidently, optimal building operations stand to benefit from the integration of multiple data sources as it relies not only in the awareness of suboptimalities but also the targeting of suboptimality causes. A building energy management toolkit incorporating multiple operational data sources would address multiple domains of energy savings and increase the flexibility of energy-saving decisions.

1.2 Motivation and objectives

While there have been major developments in the past two decades in data-driven energy monitoring and management methods, the majority are derived from a single domain of operational data, despite a variety of existing and emerging system performance data [71], [72]. The tendency to focus on a single stream of data means existing research and case studies in

building energy management toolkits tend to gravitate towards a single domain of performance data analytics such as energy benchmarking, AFDD, or OCC to name a few. There is a lack of studies which analyze the applicability of a multi-source building energy management toolkit. This paper presents a preliminary multi-source data-driven building energy management toolkit that synthesizes established data-driven approaches from the literature. The backbone of this toolkit is compiled as a Python function library stored in a public GitHub repository along with documentation, examples, and sample data. In addition to presenting the toolkit, the present capabilities of the toolkit are demonstrated using a six-storey academic building as a case study.

2. 0 Methodology

This section presents an overview of the function library with relationship to the publications forming its structure, the input data types with the relevant parameters, and its intended uses. The algorithms, literature sources, specific inputs and generated key performance indicators (KPI) of each function are presented in greater detail, as well as results from the case study, in Section 3. Figure 1 illustrates the input data types, distribution of the data, and the KPIs that each function output.

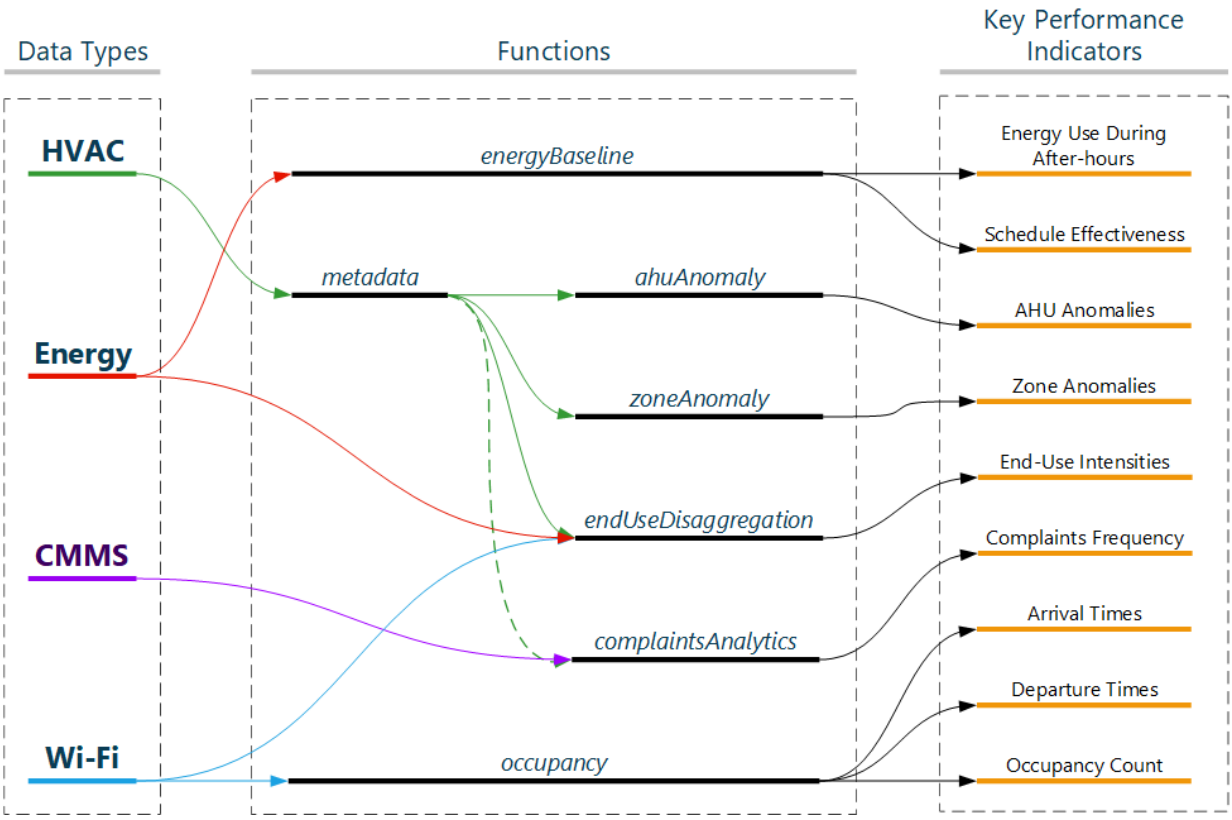

Figure 1: Overview of BEM toolkit with the distribution of data and outputted KPIs of each function.

The corresponding data types are inputted into the functions which derive their own unique KPIs. Outdoor air temperature is used by the *energyBaseline* and *complaintsAnalytics* functions, though is treated as a discrete hourly weather data source (i.e., separate from HVAC controls network data) and not explicitly shown. Note also that HVAC controls data are optional for the *complaintAnalytics* function.

Development of the BEM toolkit began with understanding the needs and challenges of the industry and the application venues for multi-source data analytics. A stakeholder's workshop titled "Designing Future Building Energy Management Tools" was organized with over 50 expert participants in Ottawa, Canada. The participants included representatives from eleven companies that specialize in data analytics for building energy management, two large building portfolio management companies, and government and university researchers. The workshop discussed the potential for additional insights from incorporating multiple data sources. For example, complaints analytics can be derived from investigating the spatiotemporal relationship between CMMS and HVAC controls data. Energy meter, occupancy, and HVAC controls data can be used to further disaggregate energy use into the building's major end-uses. Key publications addressing multi-sourced analytics applications were identified and gaps in such publications were addressed as additional contributions to the literature. Subsequently, interviews with building operators were conducted by Afroz *et al.* [73] to reveal the current functionalities of existing software tools. The findings of the workshop and interviews formed the structure of the function library which was subsequently presented to the industry stakeholders. The functions were developed to bridge the gap between information and action by providing operators with a means to quickly extract performance metrics and generate a brief and intuitive interface to inform energy-saving decisions.

The function library was prototyped in MATLAB and subsequently translated into Python, an open-source programming language. A link to the repository accompanies the submission of this paper. [1]

2.1 Operation data input

Hourly HVAC controls network trend data at the AHU- and zone-level served as inputs for five of the seven functions in Figure 1. These data are trend logs of AHU- and zone-level sensor and actuator measurements which were extracted from the BAS. The relevant data types for AHUs are

supply, return, and outdoor air temperature (T_{sa}, T_{ra}, T_{oa}), supply air pressure (P_{sa}), outdoor air damper position (S_{oa}), heating coil valve position (S_{hc}), cooling coil valve position (S_{cc}), supply fan state (S_{fan}), supply air temperature setpoint (T_{sasp}), and supply air pressure setpoint (P_{sasp}). The relevant parameters for zones are the indoor air temperature (T_{in}), VAV terminal device airflow rate (Q_{flo}) and airflow setpoint (Q_{flosp}), and perimeter heater state (S_{rad}).

Hourly building-level energy meter data for electricity, cooling, and heating energy use served as inputs for three of the functions in Figure 1. The electricity data typically represents end-uses for lighting, plug loads, fans, pumps, chiller consumption, and other equipment (e.g., elevators). The heating and cooling data represents the thermal energy transferred to the building at hourly intervals.

Two CMMS data fields, the operator description of the work order and the report time, are used as inputs for one of the functions in Figure 1.

Floor-level hourly Wi-Fi device count data acquired from an institutional IT network are used as inputs for two of the functions in Figure 1.

2.2 Intended use

The BEM toolkit is intended to provide building operators with a versatile method to address operational deficiencies by interpreting metadata, fixing hard faults, fixing soft faults and upgrading sequences, and monitoring KPIs. With the exception of the metadata inference function (*metadata*) which is intended to automate the selection of the appropriate sensor and actuator labels used to extract HVAC controls network data, each function employs a unique methodology from the existing literature and generates KPIs and visualizations which can be used to inform energy-saving decisions or monitor energy use.

The baseline energy function (*energyBaseline*) serves to illustrate the building's heating, cooling, and electricity energy use as a function of outdoor air temperature during work-hours and after-hours. The generated KPIs are intended to help building operators assess the effectiveness of current operating schedules in reducing energy consumption outside of the AHUs' operating hours

and assess the effects that fixes to hard and soft faults and changes to sequences of operation have on energy consumption.

Soft and hard AHU and VAV terminal faults may result in unintended excessive energy consumption. The AHU anomaly detection function (*ahuAnomaly*) is intended to detect anomalous operating conditions in AHUs which may be symptomatic of faults such as stuck heating coil valves, stuck cooling coil valves, leaky or stuck dampers, excessive use of perimeter heating in the economizer mode, absence of a schedule, and/or absence of an economizer mode. The generated insight is intended to help building operators focus fault correction efforts to specific AHUs and components. Similarly, the zone anomaly detection function (*zoneAnomaly*) is intended to detect anomalous zones based on temperature and airflow control errors which can help building operators isolate fault correction efforts to specific zones and VAV terminal units.

An understanding of how energy is distributed within a building may aid in fostering energy-saving decisions and may be used to isolate energy use anomalies in major end-uses. The end-use disaggregation function (*endUseDisaggregation*) further separates bulk electricity, heating, and cooling consumption into six end-uses: electricity consumption into lighting and plug-in equipment loads, distribution, and chillers, heating consumption into perimeter heating and AHU heating coils, and cooling consumption into AHU cooling coils. This function is intended to calculate energy use intensities (EUIs) at a higher end-use resolution and help operators understand the flow of energy within the building's systems should end-use submetering be unavailable in their buildings.

Occupant-count patterns may be used to derive ventilation schedules that mitigate excessive energy use from overventilation, arising from an assumed constant and often overestimated occupant-count in the HVAC design phase. The occupancy function (*occupancy*) estimates occupancy-centric metrics per floor and is intended to inform building operators in refining ventilation schedules to appropriate amounts for the estimated occupancy.

Occupant feedback may be used to estimate optimal indoor temperature setpoints for certain outdoor conditions that reduce the frequency of manual setpoint changes. Setpoint changes can

impact a building's energy performance [74] which can be exacerbated with increased frequency of user-solicited changes. The complaints analytics function (*complaintsAnalytics*) extracts hot/cold related complaints and models conditions which trigger those complaints, and is intended to aid building operators in understanding what conditions give rise to thermal complaints.

Figure 2 summarizes the toolkit's intended order to address operational deficiencies and the functions' intended uses. It should be noted that the functions' KPIs and visualizations, though developed with its intended use in mind, should not be limited to its intended use. For example, though the end-use disaggregation function is intended to monitor the flow of energy within a building, it can also be used to inform fault evaluation. However, the order of operation is critical. Detecting faults without first interpreting the metadata is difficult and understanding the flow of energy in a building without first correcting hard and soft faults is a futile effort.

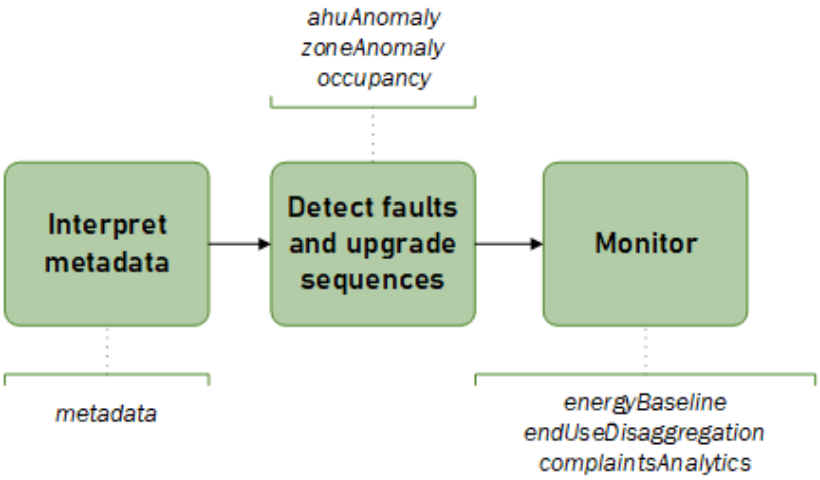

Figure 2: Flowchart depicting the BEM toolkit's intended order of operation to address operational deficiencies with the corresponding functions.

2.3 Case study

The capability of the toolkit was demonstrated on an academic building in Ottawa, Canada. Each function was employed using one or multiple streams of archived operational data accumulated over a year. The building is six-storeys high with one floor below-grade, has a gross area of 6650 m^2, accommodates a suite of classrooms, offices, meetings rooms, and labs, and is equipped with two AHUs which serve 42 thermal zones. Each zone is equipped with at least one type of perimeter heating device – VAV reheat coils and/or ceiling-mounted hydronic heaters. Cooling is provided using two chillers located on site. A district plant provides steam which passes through the

building's heat exchanger and heats hot water used in the AHUs' heating coils, VAV terminal reheat coils, and perimeter hydronic heating devices. The building has a switchover period between the heating and cooling season whereby mechanical cooling is unavailable during the heating season and space heating is unavailable during the cooling season. Two to five Wi-Fi access points are located on each of the seven floors. Hourly or sub-hourly Wi-Fi-enabled device count, HVAC control network trend, and energy meter network data were extracted, along with CMMS data, from four disparate operational databases. The case study dataset is provided along with the functions in the public GitHub repository [1].

3.0 Results and discussion

This section presents the inputs, generated KPIs and visualizations, algorithms used, assumptions and limitations, and accompanying literature which forms the basis of each function. The implementation of each function on data from the case study building is discussed along with the resultant visualizations and KPIs, as well as any potential insights.

3.1 Energy performance benchmarking (*energyBaseline* function)

Inputting energy meter data and outdoor weather data, the baseline energy function adopts the methodology described by Gunay *et al.* [18]. The KPIs generated are the schedule effectiveness and after-hours energy use, calculated separately for heating, cooling, and electricity use. The schedule effectiveness reports the complement of the ratio of the secondary slope, representing after-hours energy use rate, to the primary slope, representing workhours energy use rate. Lower values correspond to similar rates of energy use during workhours and after-hours and are symptomatic of an ineffective or outright absence of a schedule where there is minimal reduction to energy use during after-hours. The after-hours energy use computes the ratio of after-hours energy use to the total energy use separately for heating, cooling, and electricity. Lower values indicate minimal after-hours energy use while values approaching and exceeding 0.5 indicate similar or greater after-hours energy use. The energy baseline function employs the genetic algorithm to develop a modified ASHRAE Guideline 14 [75] three-parameter univariate change point model for heating, cooling, and electricity usage – with outdoor air temperature as the regressor – and estimates the unknown parameters of the models. The separation of the modified three-parameter change point model is governed by a steady-periodic weekly AHU operating schedule. Note that workhours and after-hours consumption is not representative of energy use

during and outside occupant work schedules, but rather differentiates energy use during scheduled AHU operating hours and outside scheduled AHU operating hours, respectively; the start and stop time of the operating hours are estimated using the genetic algorithm.

Collected meter data and outdoor temperature weather data from January 1st, 2019 to December 31st, 2019 from the building's three dedicated heating, cooling, and electricity meters. These data were used to demonstrate the capability of the baseline energy function. Figure 3(a) depicts the building's baseline heating energy consumption as a function of outdoor air temperature; two other similar plots were produced which depicted cooling and electricity use. The primary slope which represents the energy use rate during scheduled AHU operating hours is the steeper of the two slopes, while the shallower slope represents the energy use rate outside scheduled AHU operating hours. Figure 3(b) represents the building's predicted heating load; another two plots were generated for cooling and electricity load in the same format. The predicted loads include the average steady-periodic variation during a weekday, resulting in the minor hourly variations, and are presented at select outdoor air temperature. They can be used to assess how energy use fluctuate during the day and how outdoor air temperature affects the magnitude of the fluctuations. Since the predicted energy loads are generated using the same datasets, alterations to the baseline consumption are reflected in the resulting predicted load. Table 1 presents the generated KPIs.

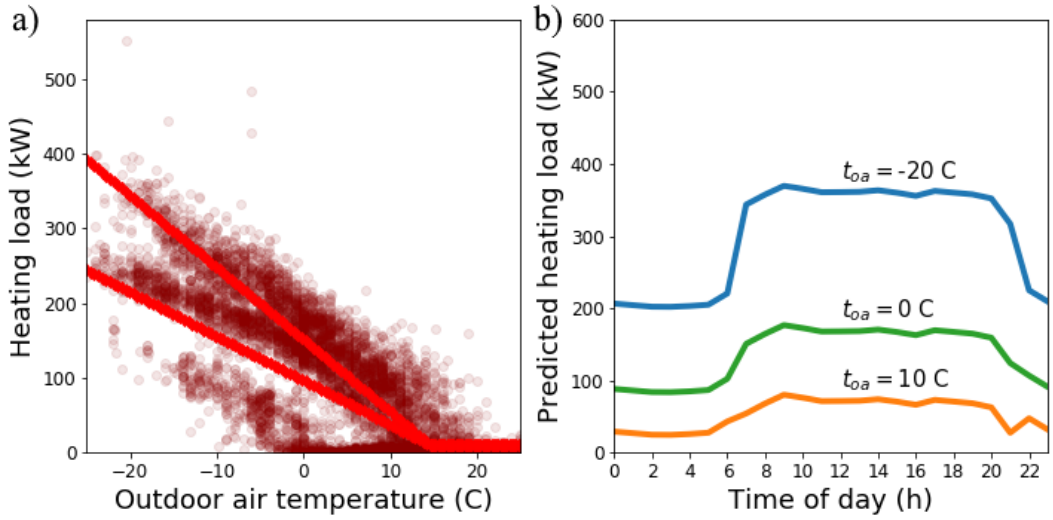

Figure 3: An illustration of the (a) modified three-parameter change point models for baseline heating energy use which minimizes CV-RMSE and (b) predicted heating energy consumption with added weekly average residuals.

*Table 1: Schedule effectiveness and after-hour energy use fraction (*energyBaseline *function KPIs).*

KPIs	Schedule effectiveness	After-hours energy use
Heating	34%	42%
Cooling	61%	12%
Electricity	18%	44%

Although the high schedule effectiveness and low after-hours energy use for cooling suggest an effective reduction in cooling energy use during after-hours in the case study building, it is unusual that any cooling energy is consumed outside the AHUs' scheduled operating hours. In this case, an overheating IT room during the cooling season was identified to have woken up the AHUs overnight (i.e., night-cycling). The issue was discussed with the facility managers and the threshold for overheating for outside schedule hours was increased from 27°C to 28°C; this behaviour has since stopped.

Electricity exhibited the lowest schedule effectiveness and highest after-hour energy use, suggesting that electricity energy use was not effectively reduced outside of the AHUs' scheduled operating hours. This is not ideal. Although a fraction of the lights remains on in corridors and multi-purpose rooms during after-hours for safety purposes, the majority operate based on motion detection and turn off automatically if no motion from occupants is detected. Other electricity end-uses such as plug loads and elevators are influenced by occupancy. The most likely cause for the high after-hours electricity use may be from chiller activity and subsequent AHU fan power usage outside the AHU's scheduled operating hours as a result of the previously mentioned overheating IT room (i.e., inappropriate night-cycling). Plug loads outside AHU operating hours would also contribute to the high after-hours electricity use (i.e., computers left on overnight, office appliances such as mini-fridges, etc.).

Heating energy use is less effectively reduced during after-hours than cooling energy use. It should be considered that once the AHUs shut off, ventilation stops and there is no need to heat or cool outdoor air. Thus, the schedule effectiveness for heating is indicative of the role of ventilation on the overall heating demand. An abnormally high heating schedule effectiveness can indicate excessive heating demand during operating hours resulting from overventilation, at least beyond ASHRAE Standard 62.1 [76]. In contrast, an abnormally low heating schedule effectiveness

indicates similar heating demands when ventilation is present during operating hours to when there is no ventilation outside operating hours. Such a case may be symptomatic of underventilation or poor envelope thermal insulative performance. In the case study building, the overheating IT room coupled with a disparate issue with the AHUs economizing in the heating mode, discussed later in subsection 3.3, caused the building to intake sub-zero outdoor air during the heating season which exacerbated perimeter heater loads outside scheduled hours.

3.2 Metadata inference for AHU and zone-level BAS labels (*metadata* function)

The metadata inference function which adopts the methodology described by Chen *et al.* [37] facilitates the metadata mapping process by classifying BAS labels into groups of the relevant sensor and actuator types, and then associating the labels to the corresponding AHU or zone [38], [40], [77]. Note that this function does not output any KPIs and serves purely to identify the labels which correspond to the required data types for HVAC controls network trend data. The function classifies labels based on a pre-defined dictionary of common tag abbreviations which was developed by extracting multiple naming conventions from over 20 buildings' BAS labels commissioned by varying control vendors. For example, T_{sa} is commonly abbreviated to 'tsa' or 'sat'. Thus, labels with tags matching one or more of the abbreviations are included in the label group for T_{sa}. However, should the labels contain unsuitable tags such as 'sp', 'stp' or 'set', to name a few, they are excluded. The edit distance for each label was computed and the least dissimilar label of each unique point type was associated to AHUs or zones. Should the labels be insufficiently descriptive and too dissimilar to be associated, the function resorts to applying the same analysis to the labels' controller address which identifies the type of device and control points. A modified Levenschtein-distance analysis as depicted in Figure 4 is employed for zone-level labels where numerical changes are weighed more heavily than alphabetical changes.

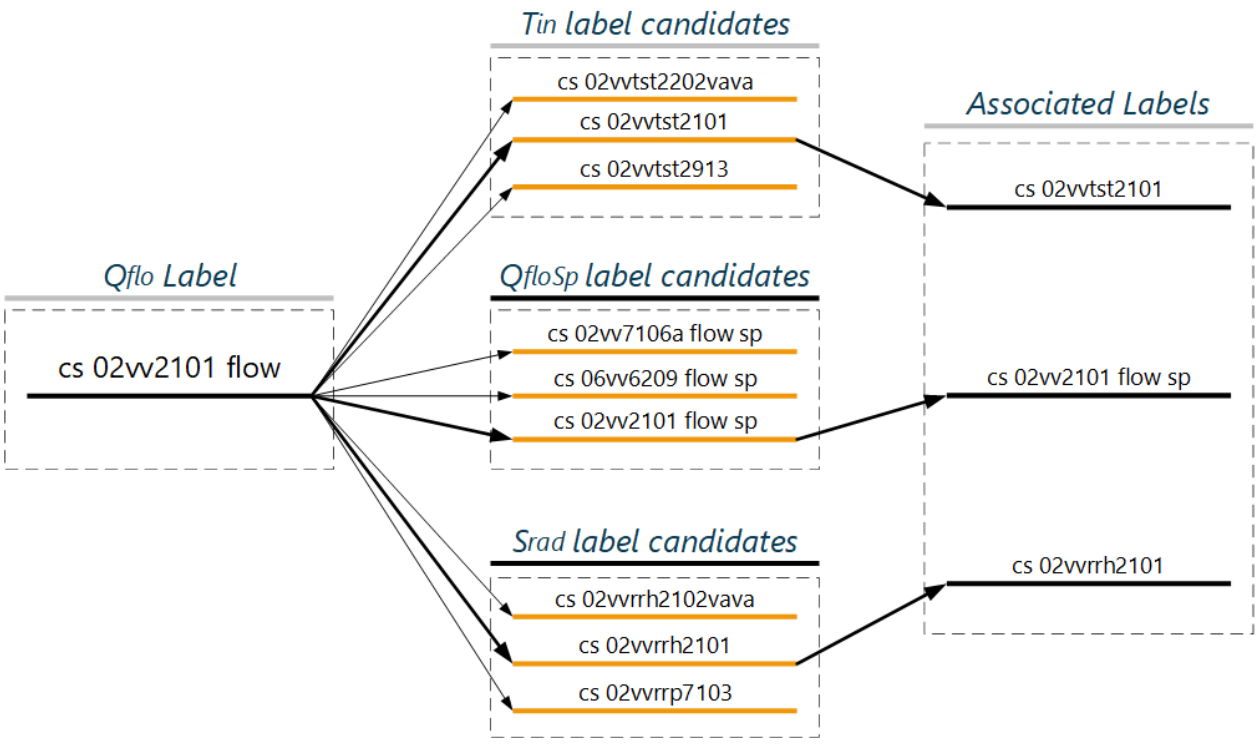

Figure 4: An illustrative example of the Levenschtein edit distance-based label association process for zone-level metadata labels.

The metadata inference function assumes that every AHU has one cooling coil with a unique label and that every zone has one airflow sensor with a unique label; the number of AHUs and zones are determined through this assumption. It is also assumed that HVAC controls data labels are associated with the AHU or zone so long as the label name or controller address are alphabetically or numerically similar (i.e., the cooling coil label for a particular AHU is similar to all other point type labels associated with that AHU). With the case study building, these assumptions resulted in inaccuracies in the metadata mapping process where one point label would be applied to multiple AHUs; these inaccuracies are expected. As such, this function is intended to be part of a semi-automated process administered by an analyst whereby review and manual revisions are allowed afterwards.

3.3 Detection of AHU anomalies (*ahuAnomaly* function)

The AHU-level anomaly detection function inputs AHU- and zone-level HVAC controls network trend data to detect common soft and hard faults in AHUs and is based on the methodology described in by Gunay *et al.* [78] and Darwazeh *et al.* [79]. The function outputs an AHU health index KPI for each AHU which yields a value of 100% when the AHU is free from the six fault

types referenced in Table 2 (three hard and three soft fault categories) and 0% when all six faults are present. The function also develops two visualizations for each AHU in a building. The first presents the AHU actuator positions and the fraction of active perimeter heater devices on a schematic demonstrating the four modes of operation described in ASHRAE Guideline 36 [80] (i.e., heating, economizer, economizer with cooling, and cooling) over outdoor air temperature, see Figure 5. The coldest, warmest, and average zone temperatures as well as the supply air temperature are superimposed. The second visualization is a set of simplified AHU diagrams which capture AHU actuators and supply, return, outdoor, and mixed air temperatures at four to six distinctive periods of operations. The fraction of the captured actuator and temperature values to the total operating duration of the AHU and average perimeter heater valve state is also displayed as in Figure 6.

The AHU-level anomaly function develops an inverse greybox model to detect common hard faults. The model predicts the supply air temperature of the AHU as a function of the outdoor and return air temperatures, outdoor air damper position, and the heating and cooling coil value positions. The parameters of this inverse model are estimated by a genetic algorithm. Detailed information about the model form and the hyperparameters of the genetic algorithm is described by Darwazeh *et al.* [79]. The hard faults detected by the function were outdoor air damper stuck (open or closed), and heating and cooling coil stuck (open or closed).

In addition to hard faults, three soft faults were detected by employing the cluster analysis-based anomaly detection approach described by Gunay and Shi [78]. The three soft faults detected by the function are excessive perimeter heating in the economizer mode, inappropriate economizer mode settings, and absence of a weekly schedule. The first soft fault is usually associated with an inappropriate supply air temperature setpoint reset approach. The second soft fault can be associated with the incorrect configuration of the split range AHU supply air temperature controller. The third fault can be due to the building not having a schedule or frequent cycling caused by a few rooms overheating beyond unoccupied indoor temperature setpoints; the former can be fixed by implementing an AHU operating schedule and the latter can be fixed by adjusting airflow and/or temperature setpoints of the VAV terminals of the overheating zones during unoccupied periods.

HVAC controls network data from January 1st, 2019 to December 31st, 2019 were used to demonstrate the function's ability to detect faults and energy use anomalies in the case study building's AHUs. The schematic in Figure 5 is the first generated visualization for one of the two AHUs in the building. The supply air temperature remains relatively constant at around 16°C and dips slightly from an outdoor air temperature of -3°C to 10°C. This is indicative of a supply air temperature setpoint reset where the supply air temperature is modulated with respect to outdoor air temperature to minimize concurrent cooling and heating. Ideally, supply air temperature is modulated to reflect the cooling and heating demands of the warmest and coldest zone respectively [81], [82]. A genetic algorithm determined the change point temperatures between the heating and economizer mode, economizer and economizer with cooling mode, and economizer with cooling and cooling mode to be about -6°C, 12°C, and 21°C, respectively.

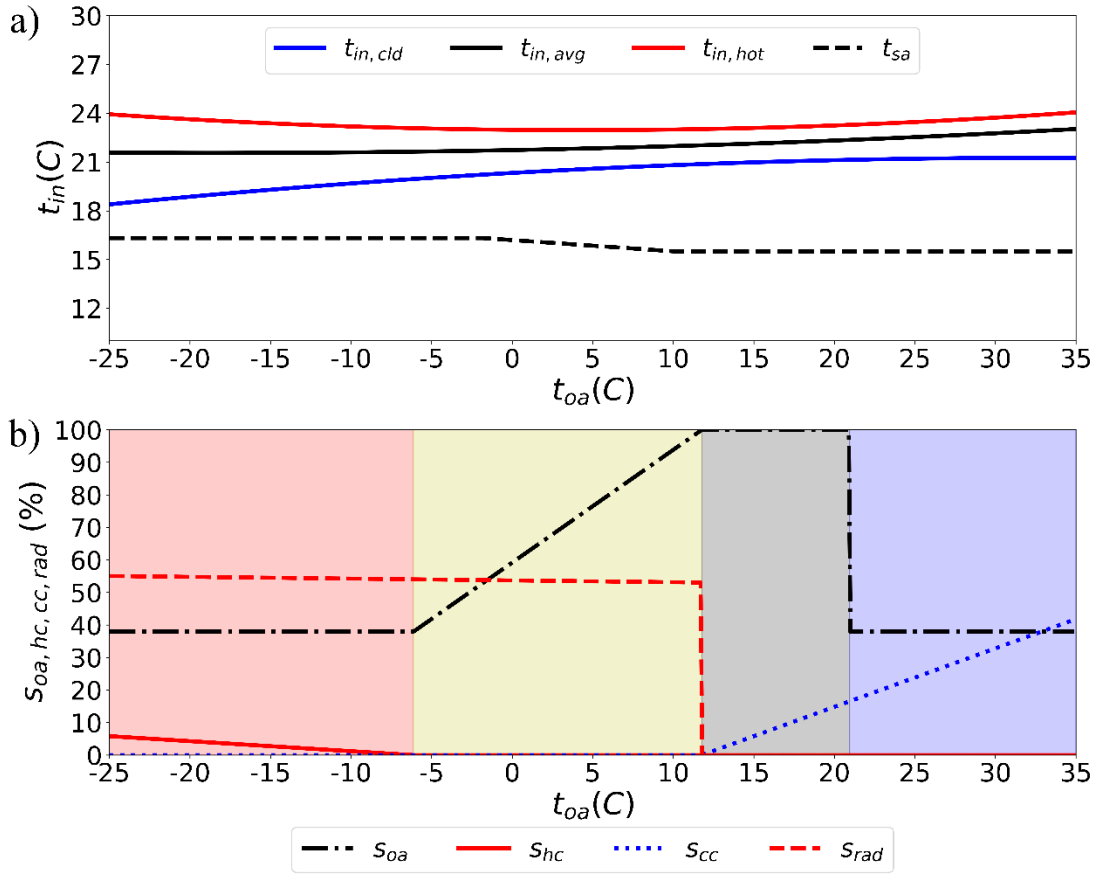

Figure 5: Schematic visualization of (a) the coldest zone, warmest zone, average zone, and supply air temperature ($t_{in,cld}$, $t_{in,hot}$, $t_{in,avg}$, and t_{sa}, respectively) with respect to outdoor air temperature, and (b) outdoor air damper, heating coil valve, cooling coil valve positions and fraction of active perimeter heater devices (s_{oa}, s_{hc}, s_{cc}, and s_{rad}, respectively) with four modes of operation

over outdoor air temperature. The AHUs' four modes of operation are represented as heating (red zone), economizer (yellow zone), economizer with cooling (grey zone), and cooling (blue zone).

Two points of concern were observed in the case study building; the first point of concern was the unusually large fraction of operating perimeter heaters while the AHU was in the economizer mode. Ideally, there is minimal to no use of the perimeter heaters in this mode since the building is trying to induce cooling; hence the outdoor air damper modulating above its minimum position in the economizer mode. Second, the valve position of the heating coil, even at the peak of the heating season, was minimal; this suggests under-utilization of the AHUs' heating coils. At -25°C, the heating coil valve position is only at about 4% open. The heating coil valve positions are expected to be significantly more open (i.e., near/at 100% [80]) at extreme cold outdoor air temperatures than what is observed. These abnormal trends would suggest an identified conflict between the economizer mode and perimeter heaters. To prevent overheating zones during the heating season, the economizer mode is engaged and subsequently the AHU heating coils shut off if the average zone temperature exceeded an overheating zone temperature threshold. However, since this threshold and the default zone temperature setpoints were identical, this threshold was frequently exceeded due to perimeter heaters which operate on reactive-based controls. The result is AHUs operating in the economizer mode in an effort to cool the seemingly overheating building but with perimeter heaters working excessively to combat the intake of sub-zero outdoor air and maintain the zone temperature setpoint. Since the default zone temperature setpoints are 22°C, the threshold for overheating in the heating season to engage the economizer mode was changed to 23.5°C from 22°C to allow the average zone temperature to slightly exceed its setpoint and differentiate from true overheating.

The second generated visualization include six diagrams for each of the case study building's two AHUs (i.e., 12 diagrams in total) which provides a visual summary of common AHU operating conditions. The k-means, Gaussian mixture, and agglomerative clustering algorithms were used to group AHU operating conditions of similar damper, valve, and temperature measurements into four to six clusters, separately for the heating and cooling seasons. The Calinski-Harabasz score was used to select the best clustering algorithm which was used to produce the diagrams. Figure 6 is one of six snapshots of one of the AHUs which characterizes 25% of the AHU's cumulative

operation. These summary diagrams can assist operating staff in interpreting the detected anomalies or in detecting other anomalies that were not detected by the function.

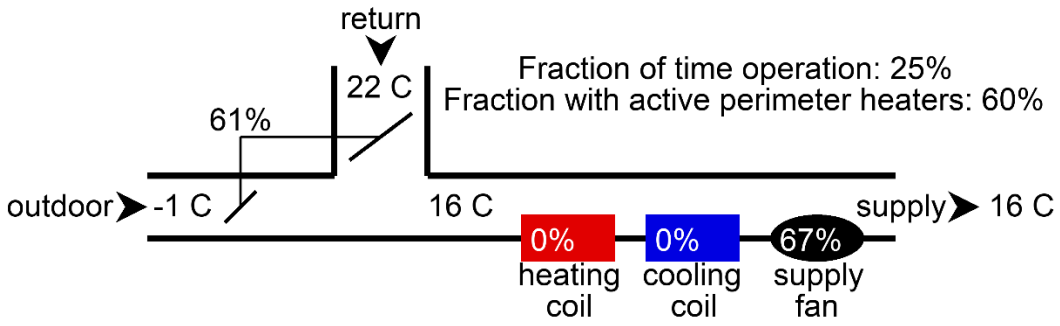

Figure 6: Example of simplified AHU diagram snapshot with AHU dampers, valve states, air temperatures, and fraction of time of operation. The fraction of active perimeters for the period of operation is also displayed.

Table 2 show the detected hard and soft faults and AHU health index. Low outdoor air was flagged in both AHUs which is typically symptomatic of an outdoor air damper that is stuck closed. However, this is more likely a result of a high fault detection threshold for outdoor air fraction bias. For the case study building, lower outdoor damper positions tend to produce lower than expected outdoor air fractions, as indicated in Figure 7; though not a fault, this resulted in an outdoor air fraction bias that is symptomatic of a stuck closed outdoor air damper. Even so, this can still prove problematic for indoor air quality purposes as outdoor air damper positions as high as 55% only supply about 20% outdoor air flow. The bias threshold is not suitable and should be reduced to avoid raising this false-positive.

*Table 2: AHU health index and summary of detected soft and hard faults (*ahuAnomaly *function KPIs)*

AHU	Health index (%)	Cooling coil	Economizer	Heating coil	Outdoor air damper	Perimeter heating in economizer mode	Schedule
1	67%	Normal	Normal	Normal	Low outdoor air	Increase T_{sasp}	Normal
2	50%	Normal	Normal	Normal	Low outdoor air	Add a low limit to economizer mode availability	No schedule

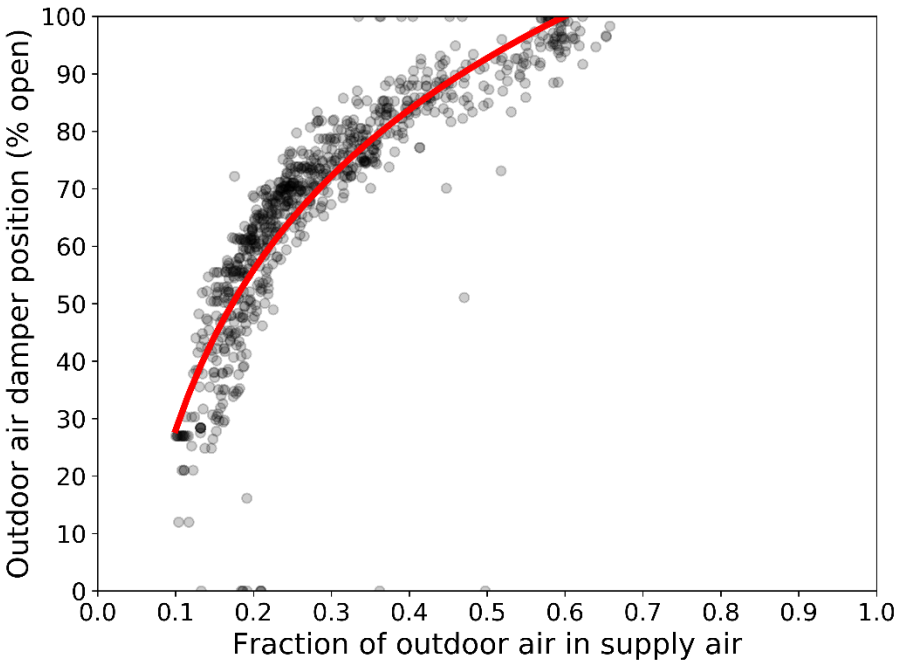

Figure 7: Visual representation of relationship between outdoor air damper position and outdoor air fraction. Lower outdoor air damper positions produce notably lower outdoor air fractions in the supply air, resulting in a low outdoor air fraction bias.

An absence of a schedule is detected in the second AHU which indicated operation of the AHU exceeding 112 hours per week (i.e., 16 hours per day); 112 hours per week is the detection threshold for this fault for this case study. This was a result of the aforementioned overheating IT room causing night-cycling. Recall that this issue has since been resolved as the threshold for heating was increased from 27°C to 28°C.

Both AHUs were flagged for anomalous perimeter heater use in the economizer mode, indicating greater than 50% fraction of active perimeter heaters in the economizer mode. For the first AHU, the change point temperature between the heating and economizer with cooling mode was estimated to be less than -5°C; it is suggested to increase the supply air temperature setpoint as an inappropriately low setpoint may exacerbate the use of perimeter heaters in the economizer mode. For the second AHU, it is suggested to add a low limit to the economizer with cooling mode availability to delay engaging the economizer with cooling mode. This issue was resolved by adding the +1.5°C deadband to differentiate true overheating from zone air temperatures being slightly above the setpoint due to perimeter heaters.

3.4 Detection of zone-level anomalies (*zoneAnomaly* function)

Per the methodology presented by Gunay and Shi [78], the zone-level anomaly function inputs the zone-level HVAC controls network trend data and groups zones with similar average seasonal errors for airflow and temperature setpoint control. The function outputs a zone health index KPI for the heating and cooling seasons separately which ranges from 0% if all zone clusters exbibit anomalous airflow control errors to 100% if no zone clusters exhibit anomalous conditions. Visualizations depicting the clustered zones with the corresponding indoor air temperature and acceptable ranges for airflow control error accompany the KPI. The function employs k-means, Gaussian mixture, and agglomerative clustering algorithms to group zones into three to five clusters, separately for the heating and cooling seasons. Of the three algorithms, the best algorithm and its resultant number of clusters is selected using the Calinski-Harabasz score and is used to produce the visualizations and KPIs. Faults are inferred should the mean zone temperature and/or mean airflow control error of a zone cluster fall beyond the pre-defined threshold for normal error. Note that this function may not be suitable for buildings with large core spaces and few perimeter heating devices; as S_{rad} is a required input for clustering for the heating season, this function is intended for building's where the majority of zone contains some form of zone-level heating.

Zone-level HVAC controls network data from January 1st, 2019 to December 31st, 2019 were used to demonstrate the zone-level anomaly detection function's ability to detect anomalous zones in the case study building. Figure 8 is the resulting visualization for the heating season analysis portion of the function; the cooling season analysis is depicted in a separate plot. The figure indicates which zone clusters suffer from airflow control and zone temperature anomalies and the severity of the anomalies. In this analysis, an airflow control error of ± 20% and an indoor air temperature of 20°C to 25°C was deemed normal. For the heating season, four clusters of zones were identified using the k-means clustering algorithm. Zone clusters C0, C1, C2, and C3 were comprised of 17, 12, 12, and 1 zone respectively. Clusters C0, C1, and C2 all fall within acceptable airflow setpoint controls errors. The zone cluster C3 deviated from the other clusters and exhibited an airflow control error of -20.4% which is marginally below the threshold for normal airflow control errors. This may be symptomatic of a stuck damper inhibiting airflow to the zone, causing a deviation between the measured airflow and airflow setpoint. If a large number of zones exhibited this issue, it may be indicative of a low supply air pressure setpoint at the AHU-level. The health

index, which quantitates zone anomalies, remains relatively high at 97.6% since only cluster C3 which contains only one zone is considered anomalous. For the summer, five clusters of zones were identified with the k-means clustering algorithm. The clusters comprised of 27, 3, 2, 4, and 6 zones, none of which exhibited anomalous conditions (within what is deemed normal). Thus, the health index remains at 100%. The breakdown of the plots and the zone health index KPIs are shown in Table 3.

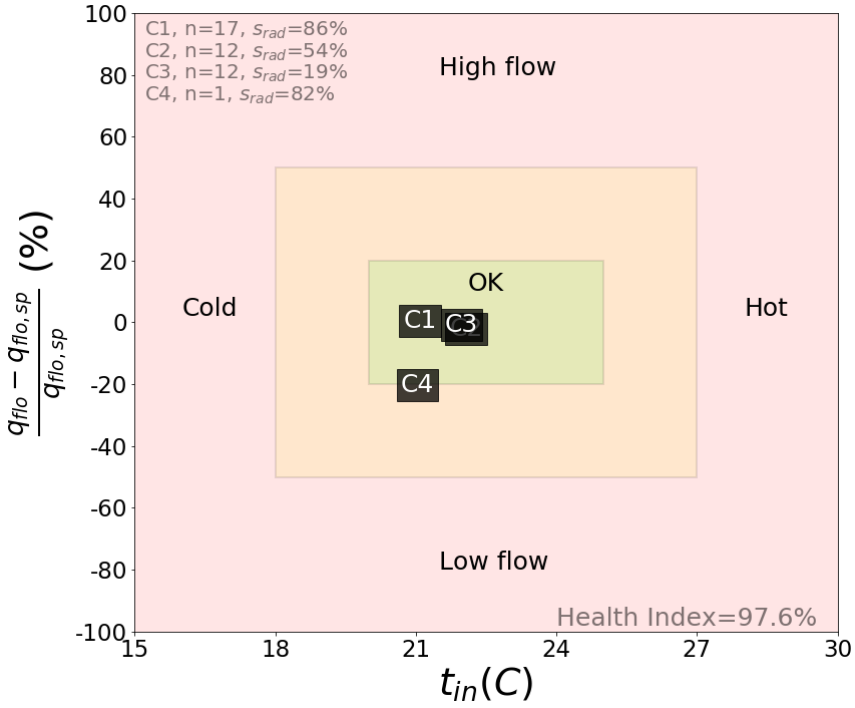

Figure 8: Clusters of zones with similar airflow control errors over indoor air temperatures for the heating season.

*Table 3: Zone health index and summary of airflow controls errors of zone clusters (*zoneAnomaly *function KPIs).*

Cluster	Heating season					Cooling season			
	# of zones	Mean T_{in} (°C)	Mean Q_{flo} error (%)	Mean S_{rad} (%)	Health index (%)	# of zones	Mean T_{in} (°C)	Mean Q_{flo} error (%)	Health index (%)
0	17	21.1	0.30	86.4		27	22.2	-0.21	
1	12	22.1	-2.07	53.7		3	22.1	-5.12	
2	12	22.0	-0.92	19.5	97.6	2	21.9	5.30	100
3	1	21.0	-20.4	82.4		4	21.6	1.83	
4	-	-	-	-		6	22.2	-1.39	

3.5 Major end-use disaggregation of bulk meter data (*endUseDisaggregation* function)

The end-use disaggregation function inputs energy meter data, AHU- and zone-level HVAC controls network trend data, and Wi-Fi device count data and is based on the methodology described by Gunay *et al.* [67] and Darwazeh *et al.* [83]. The KPIs generated by this function are the EUIs for lighting and plug-loads, distribution (i.e., pumps and fans), and chiller for electricity energy use, EUIs for perimeter heating, the AHUs' heating coils, and other appliances (i.e., domestic hot water) for heating energy use, and EUIs for the AHUs' cooling coils for cooling energy use. Visualizations depicting the weekly distribution of the major end-uses for electricity, cooling, and heating accompany the KPIs. In Gunay *et al.* [67], a genetic algorithm was used to estimate the unknown parameters of separate disaggregation models for electricity use by lighting and plug-loads, distribution, and chillers. HVAC controls network data, such as fan state, and Wi-Fi data as proxy for occupancy were used to provide contextual information to the operational state of each end-use, allowing for higher disaggregation resolution. In other words, HVAC controls network and Wi-Fi data were used to inform the disaggregation. Darwazeh *et al.* [83] extended this approach beyond electricity alone by monitoring heating and cooling energy use and using HVAC controls network data such as heating and reheat coil states as contextual information. Since lighting and plug loads, distribution, and chiller are the assumed major electricity end-uses, this function is not suitable for buildings with other significant electricity end-uses such as elevators and data centers, unless such end-uses are separated from the energy meter data prior to using the function.

As Wi-Fi data were only available in the case study building from April 23rd, 2019 until the end of the year, these data along with energy meter data and AHU- and zone-level HVAC controls network trend data from the same period were used to demonstrate the capabilities of the end-use disaggregation function in the case study building. The generated visualizations in Figure 9 represent the disaggregated EUI profiles of the major end-uses for electricity, heating, and cooling, and Table 4 shows the cumulative use for each end-use (i.e., the KPIs). Note that the due to the misaligned collection dates of data, specifically Wi-Fi data, the first 18 weeks of the plots are omitted. For electricity consumption, the lighting, plug-in, and distribution loads stay relatively consistent throughout the year whereas chiller loads transition during shoulder seasons and peak

in the cooling season. This is not unusual since chiller use is largely seasonal and lighting is not expected to vary drastically by time of year. Likewise, the relatively constant daily energy use for distribution is expected as the building requires active ventilation during occupied hours regardless of season or operating mode. For heating, domestic hot water energy consumption is consistent and is expected. However, the heavy perimeter heating energy use relative to AHU heating coils is a point of concern. The heating coils in both AHUs seem to engage minimally, even at the peak of the heating season. This anomaly was also observed in the AHU-level anomaly detection function where the fraction of active perimeter heaters was consistently high and AHU heating coil valves remained minimal even at peak heating season. Chiller use shows similar load patterns and magnitude during the peak cooling season, though one AHU sees greater use near the shoulder seasons than the other. This is expected since the building will only use one chiller until it alone is insufficient to meet the cooling demand.

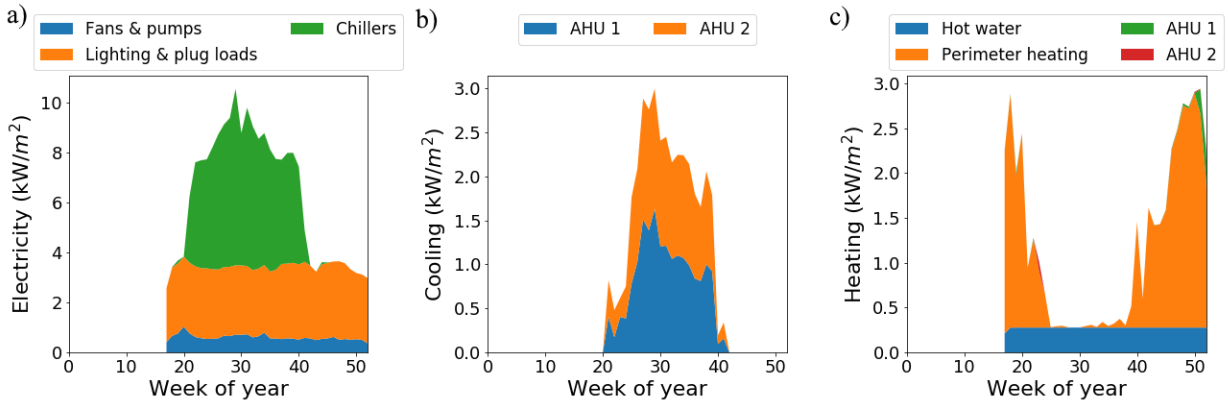

Figure 9: Weekly EUI profiles for (a) electricity, disaggregated by lighting and plug-loads, distribution, and chiller, (b) heating, disaggregated by hot water, perimeter heating, and AHU heating coils, and (c) cooling, disaggregated by AHU cooling coils.

*Table 4: Total annual EUIs of major end-uses for electricity, heating, and cooling energy use (*endUseDisaggregation *function KPIs).*

Utility	End-uses	Total annual EUI (kWh/m^2)*
Electricity	Chiller	101**
	Distribution	23.3
	Lighting & plug-in	99.6
Heating	Perimeter heating	34.3
	Heating coil (AHU 1, AHU 2)	0.754, 0.137
	Other	10.1
Cooling	Cooling coil (AHU 1, AHU 2)	18.1, 18.5

*From April 23rd, 2019 until Dec 31, 2019.

**Chiller electricity use includes use by an adjacent building.

3.6 Analysis of hot/cold complaints (*complaintsAnalytics* function)

The complaints analytics function inputs CMMS data and extracts operator comments for thermal complaints for room air temperature. This function outputs four KPIs which indicate the daily frequency of hot complaints and cold complaints generated per 1000 m^2 during both the heating and cooling seasons. This is accomplished by employing the methods developed by Dutta *et al.* [58] whereby thermal complaints which contain the terms "hot" or "cool" are extracted from the CMMS data. As this function focuses on room air temperatures, the term "water" was also included in the search criteria to identify and remove complaints regarding water temperature. Three visualizations accompany the KPIs. The first depicts the hourly and monthly distribution of hot and cold complaints. The second is a decision tree model depicting the daily frequency of hot and cold complaints based on outdoor air temperature, indoor air temperature, and time of day. The third depicts the relationship between indoor and outdoor air temperature which trigger thermal complaints. Note that the function is limited only to hot and cold complaints, and that building area must be manually inputted.

CMMS data from January 2nd, 2019 to December 23rd, 2019 were used test the capabilities of the complaints analytics function in the case study building. Figure 10 shows the first set of generated visualizations that break down the complaints by month, period of the day, and the type of complaint. A total of four thermal complaints were made: three cold complaints and a single hot complaint. Though a small sample, it seems that the complaints were made near the shoulder seasons and in the afternoons. All of the cold complaints were made in the months leading to winter while the hot complaint was reported in a month leading to summer. One possible reason for this is that the switchover periods were too delayed, which would have delayed mechanical cooling coming into the cooling season and mechanical heating into the heating season. The switchover period should then be performed earlier. It is also possible that, while switchovers were performed at correct times, unseasonably low or high outdoor air temperatures could trigger such complaints.

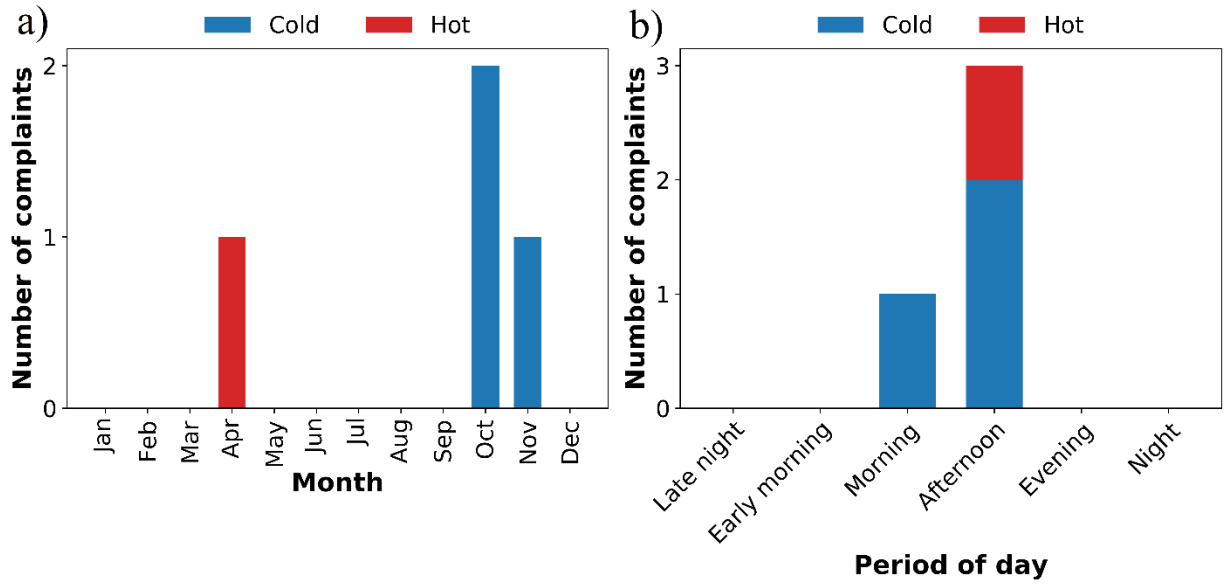

Figure 10: Breakdown of hot and cold complaints by (a) month and (b) period of day. The periods are defined as consecutive 4-hour timeslots beginning from midnight (12 am).

Table 5 shows the daily frequency of hot/cold complaints per 1000 m^2 during the summer and winter, which are the function's KPIs. Note that in this analysis, the summer months are considered from May to September inclusively; the rest are considered winter. Thus, there are no recorded complaints during the summer.

Table 5: Daily frequency of hot and cold complaints by type of complaint and season (Complaints analytics function KPIs)

	Frequency of complaints per 1000 m^2	
Type of complaint	Winter	Summer
Hot	0.0014	0
Cold	0.0041	0

The second generated visualization, seen in Figure 11, is a regression tree which models the predicted proportion of hot/cold complaints based on the time of day, day of the week, and outdoor air temperature. The criteria which lead to greater proportions of hot/cold complaints can be used to inform operations staff of the impact of indoor air temperature setpoint changes, and whether schedules should be changed. For example, should a high predicted proportion of complaints occur in the morning and at a certain outdoor air temperature, the AHU operating schedule may need to be extended earlier into the morning.

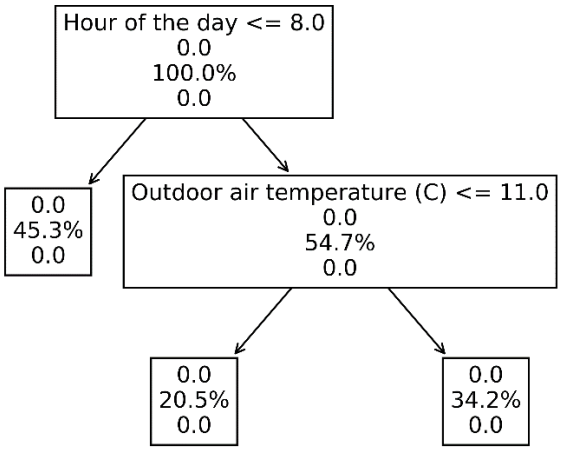

Figure 11: Regression decision tree model which predicts the proportion of the cold/hot complaints based on time of day, day of the week, and outdoor air temperature. Note that nodes branching to the left represent the predicted proportion of complaints which satisfies the criteria listed at the top of the leaf node. Due to the small sample size, the decision tree model did not split the proportion of complaints by type of day (weekend or weekday).

Figure 12 is the third generated visualization which depicts the complaints in relation to outdoor air temperature and indoor temperature. The frequency of complaints in relation to outdoor air temperature can also be used to monitor the impact of temperature setpoint changes, and whether different setpoints or revised schedules are warranted at certain outdoor air temperatures.

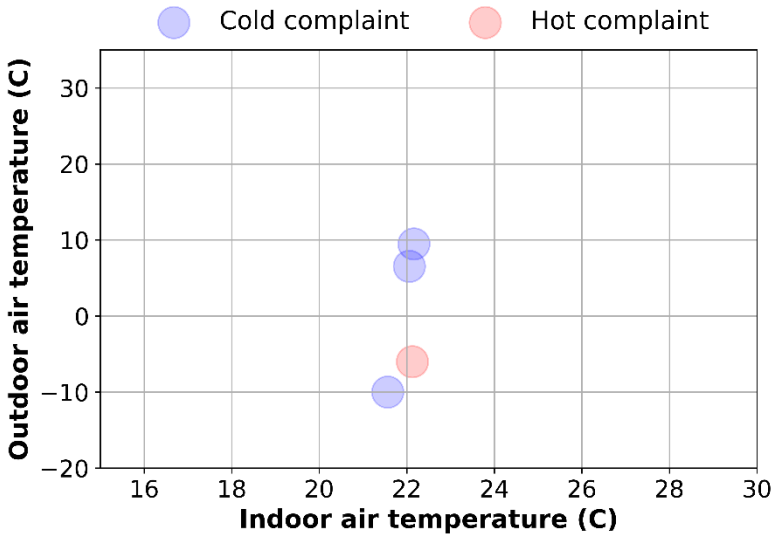

Figure 12: Visualization depicting hot and cold complaints and their relationship between outdoor and indoor air temperature.

The suitability of this function with the case study building, and its ability to generate any meaningful insight from its visualizations and KPIs, are hindered by the small sample size of hot/cold complaints. In the case study building, a small fraction of the building's occupants are

full time employees while the majority are students with intermittent presence. The transient nature of occupancy may be a deterring factor for occupants to report thermal complaints [84], [85]. A building with a more static occupancy would be expected to generate a substantially larger number of complaints, and would allow the function to provide more conclusive insights.

3.7 Occupant count estimation (*occupancy* function)

Based on the methodology presented by Hobson *et al.* [69] and Gunay *et al.* [86], the occupancy function inputs Wi-Fi device count data to generate occupant count profiles of a building for weekdays and weekends separately. The function computes the earliest expected arrival time, latest expected departure time, and highest expected occupancy per floor, which are its KPIs. Visualizations depict the 25^{th}, 50^{th}, and 75^{th} percentile occupant-count profile and the 75^{th} percentile superimposed floor-level occupant-count profile for a typical weekend and weekday. The function uses Wi-Fi device count data as proxy for occupant count. Earliest arrival times are determined by the earliest timestep whereby the 75^{th} percentile occupant count exceeded 10% of the maximum occupant count per floor. Likewise, latest departure times are determined by the latest timestep whereby the 75^{th} percentile occupant count falls below 10% of the maximum occupant count per floor. Note that the occupant-count proxy assumes 1.2 Wi-Fi devices per occupant; this relationship between occupants and devices was established in the case study building using ground truth data in a previous study [87]. This assumption may not hold true in different buildings and might even change over time as Wi-Fi device protocols evolve and the presence of Wi-Fi enabled devices increases.

Wi-Fi device count data from April 23^{rd}, 2019 to the end of the year were used to test the capabilities of the occupancy function in the case study building. Figure 13 shows the resulting plots which depict the hourly occupant count at the 75^{th}, 50^{th}, and 25^{th} percentile for a typical weekday and weekend. Figure 14 disaggregates the 75^{th} percentile occupant count per floor for weekdays and weekends. The earliest arrival time, latest departure time, and peak daily occupancy per floor KPIs are shown in Table 6.

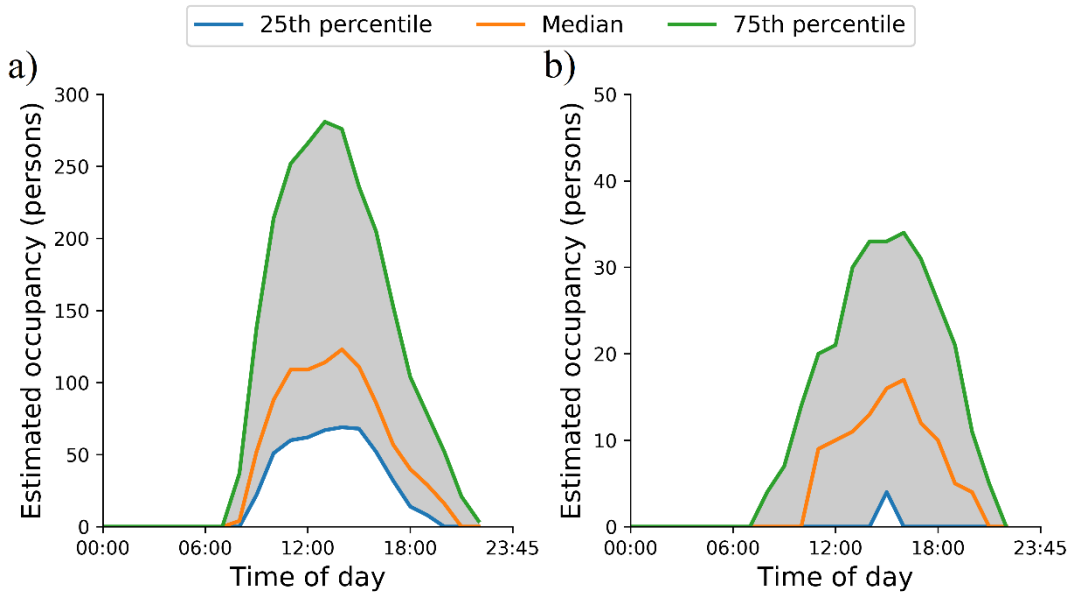

Figure 13: 25th, 50th, and 75th percentile occupant count profile for (a) weekdays and (b) weekends.

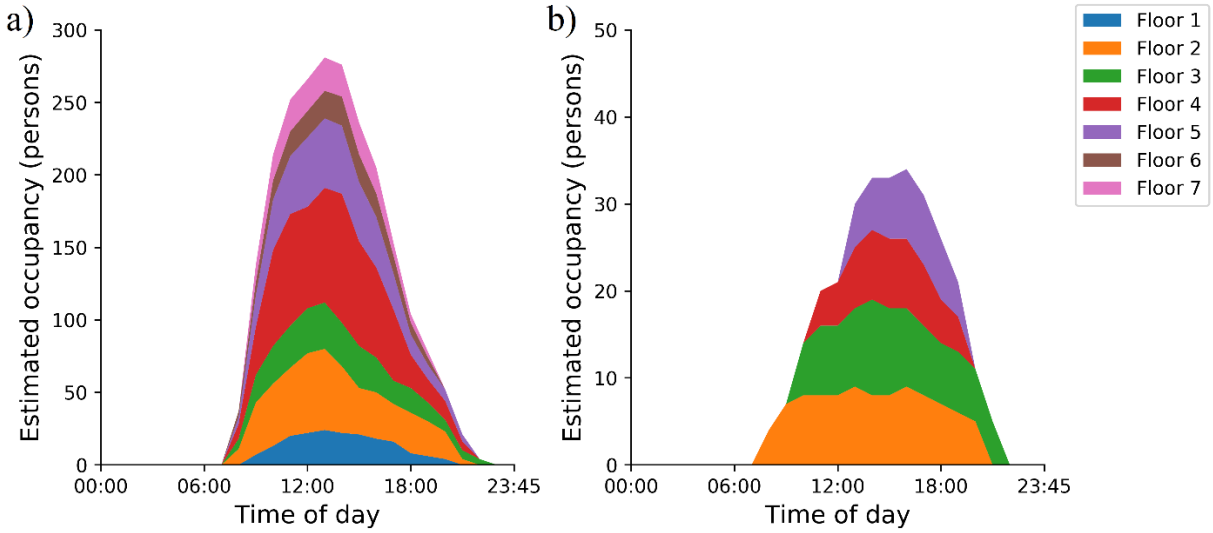

Figure 14: 75th percentile superimposed floor-level occupancy count profile for (a) weekdays and (b) weekends.

*Table 6: Earliest arrival times, latest departure times, and peak occupancy per floor for weekdays and weekends (*occupancy *function KPIs), and design occupancy per floor.*

	Earliest arrival time		Latest departure time		Typical peak daily occupancy		Design occupancy per floor
Floor	Weekday	Weekend	Weekday	Weekend	Weekday	Weekend	
1	8 am	-	7 pm	-	24	0	44
2	7 am	7 am	7 pm	7 pm	56	9	352
3	7 am	9 am	9 pm	8 pm	32	11	174
4	7 am	10 am	7 pm	6 pm	89	8	127
5	7 am	12 am	8 pm	6 pm	48	8	141
6	7 am	-	6 pm	-	20	0	98
7	8 am	-	6 pm	-	23	0	104

The total occupancy of the building during workhours peaks at 292 occupants at around noon for the typical 75th percentile workday. This is a drastic reduction from the 1040 occupants during occupied hours that was assumed during the case study building's design. The plots show the variation in occupant-count throughout the day and can be used to derive occupancy-based ventilation controls, which can modulate ventilation rates to suit the building's actual occupancy and reduce the overventilation. The generated occupancy profiles and KPIs formed the basis for an occupancy-based predictive control program which implemented different hourly outdoor air damper position profiles in the case study building's AHUs at the beginning of 2020 based on day-ahead occupant count predictions [88].

The predicted earliest arrival and latest departure time, specifically for weekends, seem inaccurate. The KPIs indicate the latest departure time for most floors to be 11 pm, although the trailing occupant-count profile towards midnight seen in Figure 14(b) more likely suggests that the latest departure time is about 4 am the next day. Furthermore, it likely appears that the earliest arrival time for weekends is about 7 am rather than midnight or 2 am as predicted by the KPIs. These inaccuracies may be caused by devices like printers and computers that are left on overnight. By late day, after peak occupancy, these devices may become artifacts and can skew the profiles. Revisions to this function should constrain earliest arrival and latest departure times within reasonable times (i.e., it is not reasonable that people arrive at 2 am or midnight). Although, a more

reliable solution can stem from establishing linear rates of daily activity of such devices and adjusting the profile to account for this relationship.

3.8 Discussion and limitations

The BEM toolkit's multifaceted analytical approach is intended to provide operators with a method to capture and monitor the propagated effects of operational deficiencies through various KPIs and visualizations. The amount of unique analytical methods under one toolkit offers a more comprehensive understanding of building operations, thus allowing for a more flexible and diverse approach in addressing deficiencies and improving operations. Underlying deficiencies are more likely to be captured since energy use anomalies and suboptimal operations undetected from one function can be detected from a number of the other functions. Furthermore, since many KPIs and visualizations are derived from the same data, underlying deficiencies can be captured from multiple unique interpretations of the data which can be consolidated to focus fault correction efforts to specific components or systems. In fact, these redundant indicators between functions are encouraged if they suggest a mutual deficiency since it strengthens the confidence of the toolkit's detection capabilities. For example, recall for the case study that the low heating schedule effectiveness KPI derived from the baseline energy function indicated excessive heating energy use outside of the AHUs' operating hours. Should analysis be limited to this KPI, a number of different root causes should be examined such as a lack of an AHU heating schedule, conflicts in the operational logic, or excessive heating demand during operating hours due to overventilation. However, Figure 5 from the AHU anomaly detection function indicated excessive use of the perimeter heating devices; this issue was also seen in Figure 9(c) from the end-use disaggregation function. Presented with this additional insight, an end-user would be compelled to investigate the relationship between excessive heating energy use and the perimeter heating devices. The root cause was determined as a conflict between the perimeter heating device setpoint and the overheating setpoint to engage the AHUs' economizer mode which led to excessive perimeter heater use; an overheating IT room propagated this issue to outside scheduled AHU operating hours. Both issues have since been resolved. Though this example demonstrates the interrelated nature of the toolkit's functions, and the benefit of multiple interpretations of the data, it also demonstrates that the toolkit's ability to generate energy-saving insight is limited by the building operator's interpretation of the generated KPIs and visualizations. The scope of the toolkit's

capability is limited to detection and monitoring of potential operational deficiencies whereas diagnosis and correction is left to the operator's discretion.

One of the inherent challenges of implementing a building energy management toolkit to multiple buildings is the varying availability and granularity of data in different buildings. Underlying factors such as HVAC setups and physical building characteristics can also affect the toolkit's ability to generate reasonable and accurate KPIs, particularly for the anomaly detection functions that rely on detection thresholds which may exclusively suit a case study building. Though this toolkit was never intended as a universal solution but rather a framework from which derivations of building energy management solutions may be fostered, its preliminary state, including its structure and methodologies, should at least demonstrate that a toolkit encompassing multiple domains of data analytics can diversify opportunities to address operational deficiencies within an intended scope of building type and use; in this case study, medium to large commercial offices. Regarding availability of data, the functions operate independent of each other such that if a lack of certain data or data quality restricts one function, other functions that do not use that data can still be implemented and generate KPIs; this adds flexibility to the toolkit's overall implementation. It is expected that not all functions will be useful for every building. For example, the complaints analytics function was not well suited for the case study building since the building is primarily occupied by students who are intermittently present and less likely to complain. In this case, a low frequency of complaints should not suggest optimal indoor air setpoints but rather that the function cannot produce conclusive insight for the building. In addition, each function was also developed to input as little data as possible to generate KPIs, even if it meant excluding data streams that were available in the case study building and could have been used to improve reliability or accuracy of the KPIs.

4.0 Conclusions and future work

The framework for a multi-source data-driven building energy management toolkit as a synthesis of established data-driven approaches from the literature has been proposed with its inputs, algorithms used, and generated visualizations and KPIs. The toolkit is intended to provide building operators with a method to address operational deficiencies such as energy use anomalies and inappropriate schedules by interpreting metadata, fixing hard fault, fixing soft faults and upgrading sequences, and monitoring KPIs. The current capability of the toolkit was demonstrated using

various disparate types of archived operational data from an academic building. Though energy use anomaly detection was discussed extensively, the toolkit's ability to produce energy benchmarking and occupancy-based analytics should not be overlooked as these insights are similarly instrumental for deriving energy-saving decisions. Should building operators capitalize on the toolkit's flexibility, the toolkit can be implemented in a wide range of different buildings.

Currently, the only interdependency between functions exists with the metadata-inferencing function. Even then, it only serves to prepare the data for input in subsequent functions. A potential benefit of using the same set of data is that the generated KPIs and visualizations may concurrently suggest the same deficiencies. Such redundancies, as demonstrated by the baseline energy, AHU anomaly detection, and end-use disaggregation functions' role in detecting a conflict between the AHUs' economizer mode and the perimeter heating devices, would add a layer of confidence to the toolkit, especially in its anomaly detection capabilities, and can minimize the likelihood of false-positive detection. Revisions to the toolkit should attempt to integrate the KPIs and develop likelihoods of true faults in addition to just simple detection. If two or more functions generate seemingly corroborative insight, the likelihood of a specific fault or number of faults would increase. By contrast, should conflicting insights exist, the likelihood would decrease. A push to refine the functions should not be limited to improving reliability but should also work to improve the robustness of the functions. Limiting data sources to what is absolutely required to generate the desired insight may not necessarily reduce the accuracy of the KPIs but would allow the toolkit to operate in buildings that lack high resolution data.

Future case studies will demonstrate the capabilities of the toolkit on other commercial and institutional buildings and the results will be disseminated to showcase its energy-saving potential and the need to further develop data-driven approaches to building energy management. Furthermore, interviews with building operators will supplement understanding of how the toolkit's generated KPIs are actually used by operators, inform the development of performance metrics and visualization, and further improve the existing capabilities of the toolkit.

References

[1] A. Markus, "Building energy management toolkit," *GitHub repository*, 2021. [Online]. Available: https://github.com/Carleton-DBOM-Research-Group/Building_energy_managment_toolkit.git.

[2] P. De Wilde, "The gap between predicted and measured energy performance of buildings: A framework for investigation," *Autom. Constr.*, vol. 41, pp. 40–49, May 2014, doi: 10.1016/j.autcon.2014.02.009.

[3] H. P. Tuniki and P. Gultekin-Bicer, "A Comparative Case Study Approach: Identifying the Discrepancy between Energy Performance Results."

[4] B. Bordass and W. B. Associates, "Energy Performance of Non-Domestic Buildings: Closing the Credibility Gap."

[5] C. van Dronkelaar, M. Dowson, C. Spataru, and D. Mumovic, "A Review of the Regulatory Energy Performance Gap and Its Underlying Causes in Non-domestic Buildings," *Front. Mech. Eng.*, vol. 1, p. 17, Jan. 2016, doi: 10.3389/fmech.2015.00017.

[6] C. van Dronkelaar, M. Dowson, C. Spataru, E. Burman, and D. Mumovic, "Quantifying the Underlying Causes of a Discrepancy Between Predicted and Measured Energy Use," *Front. Mech. Eng.*, vol. 5, p. 20, May 2019, doi: 10.3389/fmech.2019.00020.

[7] A. C. Menezes, A. Cripps, D. Bouchlaghem, and R. Buswell, "Predicted vs. actual energy performance of non-domestic buildings: Using post-occupancy evaluation data to reduce the performance gap," *Appl. Energy*, vol. 97, pp. 355–364, Sep. 2012, doi: 10.1016/j.apenergy.2011.11.075.

[8] T. Ramesh, R. Prakash, and K. K. Shukla, "Life cycle energy analysis of buildings: An overview," *Energy and Buildings*, vol. 42, no. 10. Elsevier Ltd, pp. 1592–1600, 01-Oct-2010, doi: 10.1016/j.enbuild.2010.05.007.

[9] S. Katipamula *et al.*, "Small- and Medium-Sized Commercial Building Monitoring and Controls Needs: A Scoping Study," Richland, WA (United States), Oct. 2012.

[10] L. Pérez-Lombard, J. Ortiz, and C. Pout, "A review on buildings energy consumption information," *Energy Build.*, vol. 40, no. 3, pp. 394–398, Jan. 2008, doi: 10.1016/j.enbuild.2007.03.007.

[11] B. Dong, Z. O'Neill, and Z. Li, "A BIM-enabled information infrastructure for building energy Fault Detection and Diagnostics," *Autom. Constr.*, vol. 44, pp. 197–211, Aug. 2014,

doi: 10.1016/j.autcon.2014.04.007.

[12] A. Ghahramani, S. A. Karvigh, and B. Becerik-Gerber, "HVAC system energy optimization using an adaptive hybrid metaheuristic," *Energy Build.*, vol. 152, pp. 149–161, Oct. 2017, doi: 10.1016/j.enbuild.2017.07.053.

[13] K. W. Roth, P. Llana, M. Feng, D. Westphalen, and M. Y. Feng, "The Energy Impact of Faults in U.S. Commercial Buildings," 2004.

[14] E. Mills *et al.*, "THE COST-EFFECTIVENESS OF COMMERCIAL-BUILDINGS COMMISSIONING: A Meta-Analysis of Energy and Non-Energy Impacts in Existing Buildings and New Construction in the United States," 2004.

[15] T. Abuimara, B. Gunay, A. Abdelalim, M. Ouf, and S. Gilani, *Modelling Occupants in Buildings: Stakeholders' Workshop on Current Barriers, Challenges and Needs*. 2018.

[16] C. Miller *et al.*, "The Building Data Genome Project 2, energy meter data from the ASHRAE Great Energy Predictor III competition," *Sci. Data*, vol. 7, no. 1, p. 368, 2020, doi: 10.1038/s41597-020-00712-x.

[17] Y. Zhang, Z. O'Neill, B. Dong, and G. Augenbroe, "Comparisons of inverse modeling approaches for predicting building energy performance," *Build. Environ.*, vol. 86, pp. 177–190, Apr. 2015, doi: 10.1016/j.buildenv.2014.12.023.

[18] H. Burak Gunay, W. Shen, G. Newsham, and A. Ashouri, "Detection and interpretation of anomalies in building energy use through inverse modeling," *Sci. Technol. Built Environ.*, vol. 25, no. 4, pp. 488–503, Apr. 2019, doi: 10.1080/23744731.2019.1565550.

[19] Z. O'Neill and C. O'Neill, "Development of a probabilistic graphical model for predicting building energy performance," *Appl. Energy*, vol. 164, pp. 650–658, Feb. 2016, doi: 10.1016/j.apenergy.2015.12.015.

[20] M. L. Marceau and R. Zmeureanu, "Nonintrusive load disaggregation computer program to estimate the energy consumption of major end uses in residential buildings," *Energy Convers. Manag.*, vol. 41, no. 13, pp. 1389–1403, Sep. 2000, doi: 10.1016/S0196-8904(99)00173-9.

[21] E. Mocanu, P. H. Nguyen, and M. Gibescu, "Energy disaggregation for real-time building flexibility detection," in *IEEE Power and Energy Society General Meeting*, 2016, vol. 2016-November, doi: 10.1109/PESGM.2016.7741966.

[22] K. Basu, V. Debusschere, A. Douzal-Chouakria, and S. Bacha, "Time series distance-based

methods for non-intrusive load monitoring in residential buildings," *Energy Build.*, vol. 96, pp. 109–117, Jun. 2015, doi: 10.1016/j.enbuild.2015.03.021.

[23] H. Akbari and S. J. Konopacki, "Application of an end-use disaggregation algorithm for obtaining building energy-use data," *J. Sol. Energy Eng. Trans. ASME*, vol. 120, no. 3, pp. 205–210, Aug. 1998, doi: 10.1115/1.2888070.

[24] Y. Ji, P. Xu, and Y. Ye, "HVAC terminal hourly end-use disaggregation in commercial buildings with Fourier series model," *Energy Build.*, vol. 97, pp. 33–46, Jun. 2015, doi: 10.1016/j.enbuild.2015.03.048.

[25] B. Doherty and K. Trenbath, "Device-level plug load disaggregation in a zero energy office building and opportunities for energy savings," *Energy Build.*, vol. 204, p. 109480, Dec. 2019, doi: 10.1016/j.enbuild.2019.109480.

[26] Y. Li and Z. O'Neill, "A critical review of fault modeling of HVAC systems in buildings," *Building Simulation*, vol. 11, no. 5. Tsinghua University Press, pp. 953–975, 01-Oct-2018, doi: 10.1007/s12273-018-0458-4.

[27] Z. Shi and W. O'Brien, "Development and implementation of automated fault detection and diagnostics for building systems: A review," *Automation in Construction*, vol. 104. Elsevier B.V., pp. 215–229, 01-Aug-2019, doi: 10.1016/j.autcon.2019.04.002.

[28] W. Kim and S. Katipamula, "A review of fault detection and diagnostics methods for building systems," *Sci. Technol. Built Environ.*, vol. 24, no. 1, pp. 3–21, Jan. 2018, doi: 10.1080/23744731.2017.1318008.

[29] S. Katipamula and M. R. Brambley, "Review article: Methods for fault detection, diagnostics, and prognostics for building systems—a review, part II," *HVAC R Res.*, vol. 11, no. 2, pp. 169–187, 2005, doi: 10.1080/10789669.2005.10391133.

[30] H. Burak Gunay, W. Shen, and G. Newsham, "Data analytics to improve building performance: A critical review," *Automation in Construction*, vol. 97. Elsevier B.V., pp. 96–109, 01-Jan-2019, doi: 10.1016/j.autcon.2018.10.020.

[31] A. Afram and F. Janabi-Sharifi, "Theory and applications of HVAC control systems - A review of model predictive control (MPC)," *Building and Environment*, vol. 72. Elsevier Ltd, pp. 343–355, 01-Feb-2014, doi: 10.1016/j.buildenv.2013.11.016.

[32] S. Prívara, J. Široký, L. Ferkl, and J. Cigler, "Model predictive control of a building heating system: The first experience," *Energy Build.*, vol. 43, no. 2–3, pp. 564–572, Feb. 2011, doi:

10.1016/j.enbuild.2010.10.022.

[33] J. Ma, J. Qin, T. Salsbury, and P. Xu, “Demand reduction in building energy systems based on economic model predictive control,” *Chem. Eng. Sci.*, vol. 67, no. 1, pp. 92–100, Jan. 2012, doi: 10.1016/j.ces.2011.07.052.

[34] J. Široký, F. Oldewurtel, J. Cigler, and S. Prívara, “Experimental analysis of model predictive control for an energy efficient building heating system,” *Appl. Energy*, vol. 88, no. 9, pp. 3079–3087, Sep. 2011, doi: 10.1016/j.apenergy.2011.03.009.

[35] M. S. Mirnaghi and F. Haghighat, “Fault detection and diagnosis of large-scale HVAC systems in buildings using data-driven methods: A comprehensive review,” *Energy Build.*, vol. 229, p. 110492, Sep. 2020, doi: 10.1016/j.enbuild.2020.110492.

[36] P. A. Mathew, L. N. Dunn, M. D. Sohn, A. Mercado, C. Custudio, and T. Walter, “Big-data for building energy performance: Lessons from assembling a very large national database of building energy use,” *Appl. Energy*, vol. 140, pp. 85–93, Feb. 2015, doi: 10.1016/j.apenergy.2014.11.042.

[37] L. Chen, H. B. Gunay, Z. Shi, W. Shen, and X. Li, “A Metadata Inference Method for Building Automation Systems With Limited Semantic Information,” *IEEE Trans. Autom. Sci. Eng.*, pp. 1–13, May 2020, doi: 10.1109/tase.2020.2990566.

[38] A. A. Bhattacharya, D. Hong, D. Culler, J. Ortiz, K. Whitehouse, and E. Wu, “Automated metadata construction to support portable building applications,” in *BuildSys 2015 - Proceedings of the 2nd ACM International Conference on Embedded Systems for Energy-Efficient Built*, 2015, pp. 3–12, doi: 10.1145/2821650.2821667.

[39] J.-P. Calbimonte, Z. Yan, H. Jeung, O. Corcho, and K. Aberer, “Deriving semantic sensor metadata from raw measurements,” in *Proceedings of the 5th International Workshop on Semantic Sensor Networks at ISWC*, 2012, vol. 904, no. CONF, pp. 33–48.

[40] J. Gao, J. Ploennigs, and M. Bergés, “A data-driven meta-data inference framework for building automation systems,” in *BuildSys 2015 - Proceedings of the 2nd ACM International Conference on Embedded Systems for Energy-Efficient Built*, 2015, pp. 23–32, doi: 10.1145/2821650.2821670.

[41] W. Wang, J. Chen, T. Hong, and N. Zhu, “Occupancy prediction through Markov based feedback recurrent neural network (M-FRNN) algorithm with WiFi probe technology,” *Build. Environ.*, vol. 138, pp. 160–170, Jun. 2018, doi: 10.1016/j.buildenv.2018.04.034.

[42] W. Wang, J. Chen, and T. Hong, "Occupancy prediction through machine learning and data fusion of environmental sensing and Wi-Fi sensing in buildings," *Autom. Constr.*, vol. 94, pp. 233–243, Oct. 2018, doi: 10.1016/j.autcon.2018.07.007.

[43] Z. Wang, T. Hong, M. A. Piette, and M. Pritoni, "Inferring occupant counts from Wi-Fi data in buildings through machine learning," *Build. Environ.*, vol. 158, pp. 281–294, Jul. 2019, doi: 10.1016/j.buildenv.2019.05.015.

[44] Y. Zhao, W. Zeiler, G. Boxem, and T. Labeodan, "Virtual occupancy sensors for real-time occupancy information in buildings," *Build. Environ.*, vol. 93, no. P2, pp. 9–20, Nov. 2015, doi: 10.1016/j.buildenv.2015.06.019.

[45] E. Longo, A. E. C. Redondi, and M. Cesana, "Accurate occupancy estimation with WiFi and bluetooth/BLE packet capture," *Comput. Networks*, vol. 163, p. 106876, Nov. 2019, doi: 10.1016/j.comnet.2019.106876.

[46] A. Williams, B. Atkinson, K. Garbesi, E. Page, and F. Rubinstein, "Lighting controls in commercial buildings," *LEUKOS - J. Illum. Eng. Soc. North Am.*, vol. 8, no. 3, pp. 161–180, Jan. 2012, doi: 10.1582/LEUKOS.2012.08.03.001.

[47] Z. Nagy, F. Y. Yong, M. Frei, and A. Schlueter, "Occupant centered lighting control for comfort and energy efficient building operation," *Energy Build.*, vol. 94, pp. 100–108, May 2015, doi: 10.1016/j.enbuild.2015.02.053.

[48] G. Lowry, "Energy saving claims for lighting controls in commercial buildings," *Energy and Buildings*, vol. 133. Elsevier Ltd, pp. 489–497, 01-Dec-2016, doi: 10.1016/j.enbuild.2016.10.003.

[49] S. Schiavon and A. K. Melikov, "Energy saving and improved comfort by increased air movement," *Energy Build.*, vol. 40, no. 10, pp. 1954–1960, Jan. 2008, doi: 10.1016/j.enbuild.2008.05.001.

[50] S. Naylor, M. Gillott, and T. Lau, "A review of occupant-centric building control strategies to reduce building energy use," *Renewable and Sustainable Energy Reviews*, vol. 96. Elsevier Ltd, pp. 1–10, 01-Nov-2018, doi: 10.1016/j.rser.2018.07.019.

[51] A. Aswani, N. Master, J. Taneja, D. Culler, and C. Tomlin, "Reducing transient and steady state electricity consumption in HVAC using learning-based model-predictive control," *Proc. IEEE*, vol. 100, no. 1, pp. 240–253, 2012, doi: 10.1109/JPROC.2011.2161242.

[52] S. Goyal, H. A. Ingley, and P. Barooah, "Occupancy-based zone-climate control for energy-

efficient buildings: Complexity vs. performance," *Appl. Energy*, vol. 106, pp. 209–221, Jun. 2013, doi: 10.1016/j.apenergy.2013.01.039.

[53] J. Y. Park *et al.*, "A critical review of field implementations of occupant-centric building controls," *Building and Environment*, vol. 165. Elsevier Ltd, p. 106351, 01-Nov-2019, doi: 10.1016/j.buildenv.2019.106351.

[54] H. Zou, Y. Zhou, H. Jiang, S. C. Chien, L. Xie, and C. J. Spanos, "WinLight: A WiFi-based occupancy-driven lighting control system for smart building," *Energy Build.*, vol. 158, pp. 924–938, Jan. 2018, doi: 10.1016/j.enbuild.2017.09.001.

[55] B. Balaji, J. Xu, A. Nwokafor, R. Gupta, and Y. Agarwal, "Sentinel: occupancy based HVAC actuation using existing WiFi infrastructure within commercial buildings," in *Proceedings of the 11th ACM Conference on Embedded Networked Sensor Systems*, 2013, pp. 1–14.

[56] B. W. Hobson, D. Lowcay, H. B. Gunay, A. Ashouri, and G. R. Newsham, "Opportunistic occupancy-count estimation using sensor fusion: A case study," *Build. Environ.*, vol. 159, p. 106154, Jul. 2019, doi: 10.1016/j.buildenv.2019.05.032.

[57] R. A. Martin, C. C. Federspiel, D. M. Auslander, and A. Dean, "Supervisory Control for Energy Savings and Thermal Comfort in Commercial Building HVAC Systems," 2002.

[58] S. Dutta, H. Burak Gunay, and S. Bucking, "A method for extracting performance metrics using work-order data," *Sci. Technol. Built Environ.*, vol. 26, no. 3, pp. 414–425, Mar. 2020, doi: 10.1080/23744731.2019.1693208.

[59] S. Dutta, H. B. Gunay, and S. Bucking, "A text-mining approach to extract Operational Insights from Tenant Surveys," 2020.

[60] H. B. Gunay, W. Shen, and C. Yang, "Text-mining building maintenance work orders for component fault frequency," *Build. Res. Inf.*, vol. 47, no. 5, pp. 518–533, Jul. 2019, doi: 10.1080/09613218.2018.1459004.

[61] T. Hong *et al.*, "Commercial Building Energy Saver: An energy retrofit analysis toolkit," *Appl. Energy*, vol. 159, pp. 298–309, Dec. 2015, doi: 10.1016/j.apenergy.2015.09.002.

[62] A. Costa, M. M. Keane, J. I. Torrens, and E. Corry, "Building operation and energy performance: Monitoring, analysis and optimisation toolkit," *Appl. Energy*, vol. 101, pp. 310–316, Jan. 2013, doi: 10.1016/j.apenergy.2011.10.037.

[63] T. Zhang, A. Al Zishan, and O. Ardakanian, "ODToolkit: A Toolkit for Building Occupancy

Detection," 2019, doi: 10.1145/3307772.3328280.

[64] H. Li, C. Szum, S. Lisauskas, A. Bekhit, C. Nesler, and S. C. Snyder, "Targeting Building Energy Efficiency Opportunities: An Open-source Analytical & Benchmarking Tool."

[65] A. Miller, K. Carbonnier, and M. Frankel, "Sample Municipal Portfolio Benchmarking Report: A Portfolio Analysis of Municipal Buildings in a Sample City Mark Frankel," Portland, Feb. 2017.

[66] C. Fan, D. Yan, F. Xiao, A. Li, J. An, and X. Kang, "Advanced data analytics for enhancing building performances: From data-driven to big data-driven approaches Article History," *Build. Simul. 2020*, pp. 1–22, Oct. 2020, doi: 10.1007/s12273-020-0723-1.

[67] H. Burak Gunay, Z. Shi, I. Wilton, and J. Bursill, "Disaggregation of commercial building end-uses with automation system data," *Energy Build.*, vol. 223, p. 110222, Sep. 2020, doi: 10.1016/j.enbuild.2020.110222.

[68] H. N. Rafsanjani and C. Ahn, "Linking Building Energy-Load Variations with Occupants' Energy-Use Behaviors in Commercial Buildings: Non-Intrusive Occupant Load Monitoring (NIOLM)," in *Procedia Engineering*, 2016, vol. 145, pp. 532–539, doi: 10.1016/j.proeng.2016.04.041.

[69] B. W. Hobson, H. B. Gunay, A. Ashouri, and G. R. Newsham, "Clustering and motif identification for occupancy-centric control of an air handling unit," *Energy Build.*, vol. 223, p. 110179, Sep. 2020, doi: 10.1016/j.enbuild.2020.110179.

[70] H. B. Gunay, W. Shen, G. Newsham, and A. Ashouri, "Modelling and analysis of unsolicited temperature setpoint change requests in office buildings," *Build. Environ.*, vol. 133, pp. 203–212, Apr. 2018, doi: 10.1016/j.buildenv.2018.02.025.

[71] W. J. N. Turner, A. Staino, and B. Basu, "Residential HVAC fault detection using a system identification approach," *Energy Build.*, vol. 151, pp. 1–17, 2017, doi: 10.1016/j.enbuild.2017.06.008.

[72] C. Fan, F. Xiao, C. Yan, C. Liu, Z. Li, and J. Wang, "A novel methodology to explain and evaluate data-driven building energy performance models based on interpretable machine learning," *Appl. Energy*, vol. 235, pp. 1551–1560, Feb. 2019, doi: 10.1016/j.apenergy.2018.11.081.

[73] Z. Afroz, B. W. Hobson, H. B. Gunay, W. O'Brien, and M. Kane, "How Occupants Affect Decision-Making Building Operators'," *ASHRAE J.*, vol. 62, no. November, pp. 22–30,

2020.

[74] A. Ghahramani, K. Zhang, K. Dutta, Z. Yang, and B. Becerik-Gerber, “Energy savings from temperature setpoints and deadband: Quantifying the influence of building and system properties on savings,” *Appl. Energy*, vol. 165, pp. 930–942, Mar. 2016, doi: 10.1016/j.apenergy.2015.12.115.

[75] American Society of Heating Refrigerating and Air-Conditioning Engineers Inc, *ASHRAE Guideline 14-2014*. 2014.

[76] American Society of Heating Refrigerating and Air-Conditioning Engineers Inc, *ASHRAE Standard 62.1-2007: Ventilation for Acceptable Indoor Air Quality*. 2007.

[77] J. Koh, B. Balaji, D. Sengupta, J. McAuley, R. Gupta, and Y. Agarwal, “Scrabble: Transferrable semi-automated semantic metadata normalization using intermediate representation,” in *BuildSys 2018 - Proceedings of the 5th Conference on Systems for Built Environments*, 2018, vol. 18, pp. 11–20, doi: 10.1145/3276774.3276795.

[78] H. B. Gunay and Z. Shi, “Cluster analysis-based anomaly detection in building automation systems,” *Energy Build.*, vol. 228, p. 110445, Dec. 2020, doi: 10.1016/j.enbuild.2020.110445.

[79] D. Darwazeh, B. Gunay, and J. Duquette, “Development of Inverse Greybox Model-Based Virtual Meters for Air Handling Units,” *IEEE Trans. Autom. Sci. Eng.*, pp. 1–14, Jul. 2020, doi: 10.1109/tase.2020.3005888.

[80] American Society of Heating Refrigerating and Air-Conditioning Engineers Inc, “ASHRAE Guideline 36-2018,” *ASHRAE*, 2018.

[81] L. Wang, P. Mathew, and X. Pang, “Uncertainties in energy consumption introduced by building operations and weather for a medium-size office building,” *Energy Build.*, vol. 53, pp. 152–158, Oct. 2012, doi: 10.1016/j.enbuild.2012.06.017.

[82] H. B. Gunay, G. Newsham, A. Ashouri, and I. Wilton, “Deriving sequences of operation for air handling units through building performance optimization,” *J. Build. Perform. Simul.*, vol. 13, no. 5, pp. 501–515, Sep. 2020, doi: 10.1080/19401493.2020.1793221.

[83] D. Darwazeh, J. Duquette, and B. Gunay, “Virtual metering of heat supplied by hydronic perimeter heaters in variable air volume zones,” in *Proceedings of the 5th International Workshop on Non-Intrusive Load Monitoring*, 2020, pp. 49–53, doi: 10.1145/3427771.3429389.

[84] C. C. Federspiel, “Predicting the frequency and cost of hot and cold complaints in buildings,” *HVAC R Res.*, vol. 6, no. 4, pp. 289–305, 2000, doi: 10.1080/10789669.2000.10391418.

[85] C. C. Federspiel, R. A. Martin, and H. Yan, “Recalibration of the complaint prediction model,” *HVAC R Res.*, vol. 10, no. 2, pp. 179–200, 2004, doi: 10.1080/10789669.2004.10391098.

[86] H. B. Gunay, W. O’Brien, I. Beausoleil-Morrison, W. Shen, G. Newsham, and I. Macdonald, “The effect of zone level occupancy characteristics on adaptive controls,” in *15th International Conference of the International Building Performance Simulation Association, San Francisco, CA, USA*, 2017.

[87] A. Ashouri, G. R. Newsham, Z. Shi, and H. B. Gunay, “Day-ahead Prediction of Building Occupancy using WiFi Signals,” in *IEEE International Conference on Automation Science and Engineering*, 2019, vol. 2019-August, pp. 1237–1242, doi: 10.1109/COASE.2019.8843224.

[88] B. W. Hobson, H. B. Gunay, A. Ashouri, and G. R. Newsham, “Occupancy-based predictive control of an outdoor air intake damper: A case study,” *Proc. IBPSA-Canada eSim 2021 Conf.*, 2021.

Declaration of interests

☒ The authors declare that they have no known competing financial interests or personal relationships that could have appeared to influence the work reported in this paper.

☐The authors declare the following financial interests/personal relationships which may be considered as potential competing interests:
